# Drought Trend Assessment Using Multi-Temporal Satellite products and In-Situ Data for Amhara Region, Ethiopia

MASTAWESHA MISGANAW ENGDAW
March, 2014

SUPERVISORS:
Dr. B.H.P. Maathuis
M.Sc. Ir. G.N. Parodi

# DROUGHT TREND ASSESSMENT USING MULTI-TEMPORAL SATELLITE PRODUCTS AND IN-SITU DATA FOR AMHARA REGION, ETHIOPIA

MASTAWESHA MISGANAW ENGDAW
Enschede, The Netherlands, March, 2014

Thesis submitted to the Faculty of Geo-Information Science and Earth Observation of the University of Twente in partial fulfilment of the requirements for the degree of Master of Science in Geo-information Science and Earth Observation.
Specialization: WREM

SUPERVISORS:
Dr. B.H.P. Maathuis
M.Sc. Ir. G.N. Parodi

THESIS ASSESSMENT BOARD:
Prof. Dr. Ing. W. Verhoef (Chair)
Dr. H. van der Kwast (External Examiner, UNESCO-IHE Delft)

# ABSTRACT

Drought has been causing serious damage to the socio-economic development of Ethiopia as a nation. Specifically for Amhara region where this study is conducted, remembering the most severe droughts happened in 1974 and 1984 is enough to know to what extent drought related studies are important. Long term monthly in-situ rainfall data is used to see the spatial and temporal distribution of rainfall over the region. The results showed that the east and north-eastern part of the region receive less rainfall and are more drought prone. For some rainfall stations, both the in-situ and satellite derived the climatology over thirty years indicated that the rainfall pattern is bimodal (March to May and June to October) only for some parts of the region (mainly Combolcha and Debre Birhan) while other have single and relatively extended rainfall period. The first rainy season contributes insignificant to the agricultural production and the main agricultural season analysed is therefore the "Meher", from June to October. Comparison and validation of satellite products is conducted and showed reasonable correlation for complex topography of Amhara region. This study also used dekadal resolution and different satellite products (FEWSNET RFE, FEWSNET RFE Climatology, TAMSAT RFE, MOD16 ET, MOD16 PET, eMODIS NDVI, TAMSAT climatology and FEWSNET PET) in assessing the drought. All the informations retrieved from satellite products consider land cover of the region. Regional Unmixed Mean (RUM) method of extraction of statistics is applied. Statistics are calculated for each indicator including actual, average, minimum, maximum and absolute difference average (anomalies). Drought and non-drought dekades in the growing seasons are identified if two or more selected indicators converge to the same direction for extended period of time. Accordingly, the drought events occurred in growing seasons of 2005 and 2007 are relatively low compared to drought events occurred during most of other growing seasons. Based on the area coverage, agricultural yield and population size the results presented here focus into more detail on North Gonder, but the analysis was conducted over the whole Amhara region.

Key words: drought, satellite products, dekade

# ACKNOWLEDGEMENTS

Almighty God, I am thankful for what you have been doing in my life in the past and at present, and in the future coming. This achievement would not come true if you were not on my safest side during the troubles I had. My deepest reverence goes to my first supervisor Dr. B.H.P. (Ben) Maathuis for his amazing dedication and willingness to help me. The freedom I had to meet him at any time even when he was no around, the effort he made to show me how I can solve the challenges I have been facing were unbelievable. He thought me endless willingness and motivation to help others. My deepest gratitude goes to my second supervisor M.Sc. Ir. Gabriel Parodi for the guidance and advices he has been providing me. His office was always open whenever I went. He was always willing to help me even in times he had tight schedule. Without the advices and helps of my supervisors, it would not be as easy as this much to come up with my thesis.

I am thankful for the Netherlands Fellowship Program which sponsored my study. All staff members of the Department of Water Resources were optimistic and willing to cooperate throughout the period I stayed with them and I appreciate the effort they made in one or another way. National Meteorological Agency of Ethiopia main office and regional offices had contribution in providing the meteorological data required and they deserve lots of thanks.

My father, Misganaw Engdaw you are my courage and hope. You are the one who made me who I am today. I am thankful for all advices of my personality and care. I wish all your wishes come true. My late Grandmother Mekoya Abebe, it is you who showed me love. You were my friend to whom I talked all the challenges I faced and you solved them all. You were my confidence and it is till with me even though you are not. Let God put your soul in heaven.

I do not want to forget a trouble I had which drove me crazy. It was my toughest time of my past. All day and night, wherever I was, I had been losing my concentration because of you. I would be glad if you could see me. But, I am happy today that it did not block me from what God put for me. With all its scar (I will have many yesterdays in the future so that I do not consider it as scar), I overcame it.

My friends Teshale Tadesse (Teshe), Mulugeta Tadesse (Mule), Asmelash Gebreyhannes (Asmie), Fikir Abebe, Tigist Abreham, Mafkereseb Kassahun and you all, I am thankful for the good times we had. Abebe Nigussie (Abe) and Gebremedhin Ambaw (Gee) I am thankful for the contributions you made in this achievement.

This work is dedicated to my beloved father Misganaw Engdaw.

## Contents

# LIST OF FIGURES

# LIST OF TABLES

# LIST OF ABBERVATIONS

| | |
|---|---|
| AMSU | Advanced Microwave Sounding Unit |
| ARC2 | Africa Rainfall estimate Climatology version 2 |
| AVHRR | Advanced Very High Resolution Radiometer |
| CPC | Climate Prediction Centre |
| CSA | Central Statistics Agency of Ethiopia |
| EEA | European Environment Agency |
| eMODIS | enhanced Moderate Resolution Imaging Spectrometer |
| EOS | NASA's Earth Observing System MODIS |
| EROS | U.S Geological Survey's Earth Resources Observation and Science |
| ESA | European Space Agency |
| ET | Evapotranspiration |
| ETo | Reference Evapotranspiration |
| EVI | Enhanced Vegetation Index |
| FAO | Food and Agriculture Organization of United Nations |
| FEWSNET | Famine Early Warning System Network |
| GDAL | Geospatial Data Abstraction Library |
| GDAS | Global Data Assimilation System |
| GMAO | Global Modelling and Assimilation Office of NASA |
| GOES | Geostationary Operational Environmental Satellite |
| GOFC | Global Observation of Forest Cover |
| HAR | Hargreaves |
| IDW | Invers distance weighted |
| IGBP | International Geosphere-Biosphere Program |
| ILWIS | Integrated Land and Water Information System (GIS-RS software) |
| ITCZ | Inter Tropical Convergence Zone |
| ISOD | In-Situ and Online Data Toolbox |
| JRC | Joint Research Centre |
| LAI | Leaf Area Index |
| METOP | Meteorological Operational satellite programme |
| MOD16 | MODIS Evapotranspiration |
| MSG-SEVIRI | Meteosat Second Generation- Spinning Enhanced Visible and Infrared Imager |
| NASA | National Aeronautics and Space Administration |
| NDVI | Normalized Difference Vegetation Index |
| NMA | National Meteorological Agency of Ethiopia |
| NOAA | National Oceanic and Atmospheric Administration |
| $^{o}$C | Degree centigrade |
| PET | Potential Evapotranspiration |
| RFE | Rainfall Estimate |
| RUM | Reginal Unmixed Mean |
| SPIRITS | Software for the Processing and Interpretation of Remotely Sensed Image Time Series |
| SPOT-VEGETATION | 'Système Probatoire d'Observation de la Terre or Satellite Pour l'Observation de la Terre' |
| SSM/I | Special Sensor Microwave/Imager |
| TAMSAT | Tropical Applications of Meteorology using Satellite data and ground-based observations |

| | |
|---|---|
| TERRA/AQUA MODIS | Terra and Aqua Moderate Resolution Imaging Spectrometer |
| Tmm | Long term daily mean maximum temperature for the season |
| UNEP | United Nations Environment Program |
| USAID | United States Agency for International Development |
| USGS | U.S Geological Survey |
| XML | Extensible Markup Language |

# 1. INTRODUCTION

Drought affects agricultural and livestock production and causes severe damage to the living components of the environment by disrupting the water balance of an area. Due to these problems it is causing, many scientists are focusing on "what causes it", "what methods can be used to monitor", and to "determine to what extent it is severe". The complex relationship of drought with different physical factors affect its persistence and initiation, and makes defining drought precisely difficult (Mirabbasi et al., 2013). (Badripour, 2007) defines drought as a "natural hazard that results from a deficiency of precipitation from expected or normal which, when extended over a season or longer period of time, is insufficient to meet the demands of human activities and the environment". (Chen et al., 2009) defines it in similar to the above definition but with example defined temporal scale which is months.

It occurs everywhere on earth as far as there is deviation from the normal situation. Even though the main causes behind are precipitation shortage and its variability, lacking water has also many other contributing factors and effects (Biswas et al., 2013). In addition to determining the severity, it is also challenging to know when it starts and ends. It is difficult to identify the onset and severity using a single indicator because of its creeping nature and wide spatial extent (Gadisso, 2007). It is important to incorporate all potential indicators for its occurrence in carrying out good drought assessment.

Even though Ethiopia is a country where many water bodies are available and the source of major rivers including the Blue Nile, drought is a recurrent phenomenon. The country has a long history of drought especially the drought year 1984–1985 caused death of around a million people, livestock and crop failure. Since 1970, drought has been affecting the country at least once every 10 years and it is becoming even more frequent (Gebrehiwot et al., 2011). Especially, the northern part of the country is still exposed to recurrent drought and every year millions of people are looking for food aid. In the recent years, the Kiremt comes late, starting at the end of June and ends early around September so crops receive water for short period of time during their growing season. Among 105 districts in the Amhara region, half of them are susceptible to drought and are persistently food-insecure (Gadisso, 2007). Even though the severity is varying, there has been no year when drought didn't occur in the northern part of region.

For the Amhara region where the majority of the population is depending on rainfed agriculture, drought has a long history and is still causing damages. It is essential to provide continues assessment when and where it is occurring to be prepared as early as possible. This study can be used as an input to mitigate potential effects of drought and for long term planning and management. It can also be used as background information for further studies to be conducted in the future.

## 1.1. Drought history in Ethiopia

In Ethiopia, drought occurrence and its impact is not only related to rainfall variability in space and time, it is also related with small land holdings per household, government's limited capacity to respond to environmental changes and political instabilities (especially in the past) have been contributing significantly. The famine which occurred during 1973/74 and 1984 caused death of millions of people. Undulating and steep topography of the region (mainly, north and north eastern part of the country) is unsuitable for farming and causing degradation of fertile land due to erosion processes. Lack of people's awareness in managing their farmlands with respect to the local conditions and some other factors have been leading to low levels of agricultural and livestock productivity. For different levels of drought severities happened, households have been responding by preparing themselves for the risk that would come and responding to the actual occurring drought (Gray & Mueller, 2012). There have also been drought initiated migrations of people to less drought prone areas of the country to find better locations to limit failure of agriculture and livestock production.

## 1.2. Statement of the problem

Ethiopia's economy is dependent on rainfed agriculture which is characterized by high spatial and temporal variability (Maidment et al., 2012), (Araya & Stroosnijder, 2011), (Gelassie, 2012), (Abraha, 2013). The source of water for agriculture is natural rainfall. Rather than the total amount of rainfall, significant effect has been seen from its variability. From 30 major drought occurrences in the last nine centuries, thirteen of them have severely affected the whole country (Gebrehiwot et al., 2011). All the droughts have been causing severe and complex impact on many sectors including the agricultural sector which is the backbone of the national economy. More than a million people died, millions of people starved, complete crop failure occurred, and animals died during the year 1984-1985. Millions of people relay on food aid every year. Low-lying agro-pastoral lands and central and northern highlands are parts of the country being frequently affected by drought (Gebrehiwot et al., 2011). (Ramakrishna & Demeke, 2002) indicated that the most vulnerable parts of the country are the northern and eastern parts where the study area is located.

Drought monitoring over longer periods of time, more than ten years, enables one to develop drought early warning systems (Owrangi et al., 2011). Conventional methods of drought monitoring and trend analysis using in-situ point data is tedious and time consuming (Gelassie, 2012), (Berhan et al., 2011). Satellite products are good alternatives in providing time series data in Ethiopia where ground based measurements are sparsely distributed. The course resolution of the products and the local calibration in algorithms applied still remain unsolved specially when applying to a small area (Maggioni et al., 2013).

Different studies have been conducted using satellite products and in-situ point data for Amhara region (Gelassie, 2012), (Gadisso, 2007), (Dinku et al., 2007). This study utilizes mainly satellite products in order to see the trend of drought for some dekades.

## 1.3. Research objectives

### 1.3.1. General objective

- To assess the trend of drought using selected indicators from satellite products and in-situ data for Amhara region, Ethiopia

### 1.3.2. Specific objectives

- ✓ To assess the temporal trend of drought using satellite products for the last decade in Amhara region
- ✓ To calculate reference evapotranspiration using Enku method
- ✓ To compare PET from satellite products (MOD16 and FEWSNET), and calculated PET using Enku method
- ✓ To compare rainfall climatology products from TAMSAT and ARC version 2
- ✓ To validate satellite derived rainfall products using in-situ rainfall data

## 1.4. Research questions

The objectives mentioned above, the data to be collected and the methods selected will address the following research questions:

- Is drought occurrence frequent?
- Do drought indicators relate each other in drought assessment and which indicators should be used?
- Do PET satellite products (MOD16 PET and FEWSNET PET) correlate and is there a relationship with calculated reference evapotranspiration?
- Do satellite derived rainfall products correlate with in-situ rainfall data?

# 2. LITRATURE REVIEW

## 2.1. Drought

Next to floods (11%), drought (7.5%) is the second most widely distributed disaster on earth's land (Nagarajan, 2010). Global damage of drought per annum is estimated to be $6-$8 billion (Vasiliades & Loukas, 2009). Frequency and intensity of droughts is increasing in different parts of the world (Owrangi et al., 2011). Drought is categorized into two main classes when the amount of precipitation is smaller than the normal or average amount over the region (conceptual) and identifying the severity, when it starts and ends (operational). Drought occurs when the rainfall amount is below the average or when the amount of water that evaporates from the soil and water bodies and transpiration from plants is high. Rainfall records, compared to climatology are the first evidences either drought is occurring or not, and consequently the soil moisture starts to drop if the amount of rain falling is decreasing (Nagarajan, 2010).
(Wilhite, 2007) classified drought into four groups:

- **Meteorological drought**: is the comparison to what extent the area is dry relative to normal precipitation and the period of dryness. Atmospheric conditions which cause deficiency in precipitation vary from area to area, and deficiency in precipitation is the cause for almost all drought types.
- **Hydrological drought**: is the reduction in the level of water bodies following low precipitation. Hydrological droughts occur usually following agricultural and meteorological droughts.
- **Agricultural drought**: it occurs due to high evapotranspiration demand and low soil moisture content available for plants to fulfil their water requirement. The amount of rain falling over an area contributes more to the occurrence of agricultural drought.
- **Socio-economic drought**: this occurs when demand of goods related to availability of water is higher than the supply due to long period dryness of an area. Here, dryness is also related to the amount of population. Dryness can be expressed to what extent the water available can fulfil the amount of water required by the population.

According to (Mkhabela et al., 2010)the four types of droughts mentioned above occur because of the following reasons. When precipitation for a period of time (dekadal, monthly, or seasonal) falls below the climatology, meteorological drought starts to occur. Hydrological drought occurs if shortage of precipitation leads to shortages of ground and surface water whereas agricultural drought occurs when available moisture for the successful growth of crops is not sufficient and consequently their yield reduces (Mkhabela et al., 2010). Socioeconomic drought occurs when shortage of precipitation starts to affect the economy and socio-political growth in an area. The prior available moisture determines the lag period of agricultural drought to occur after meteorological drought (Mkhabela et al., 2010).

## 2.2. Drought monitoring

Ground based measurement of evapotranspiration, rainfall and temperature are among traditional meteorological drought indicators (Steinemann et al., 2005). Rainfall is the driving factor most of these indicators (Tonini et al., 2012). Well-known indexes are developed until recent years. Standard Precipitation Index (SPI) which is merely dependent on rainfall data, has good statistical base and capacity in producing long term and short term drought impacts(McKee et al., 1993), (Belayneh et al., 2014), (Hayes et al., 1999), and is not good in agricultural drought monitoring when compared to hydrological and meteorological drought monitoring(White & Walcott, 2009), and Palmer Drought Severity Index (PDSI) (Palmer, 1965) which is important for drought monitoring for large areas are among those (Tonini et al., 2012). PDSI uses input parameters like humidity, temperature and soil (Dogan et al., 2012). According to (Tonini et al., 2012), Surface Water Supply Index (SWSI) and Palmer Hydrological Drought Severity Index (PHDI) are widely used hydrological drought indexes. Effective Drought Index (EDI) is also used in indicating when drought begin, its accumulated stress and end (Byun & Wilhite, 1999).

Remote sensing and GIS are being used for drought detection tools for analysis to provide continuous information in space and time. Remote sensing has got more attention and it is being utilized for drought monitoring. In some areas where meteorological stations are limited, remote sensing is the merely source of information. If available, it can be used in combination with in-situ data (Rhee et al., 2010). According to (Tonini et al., 2012), different drought indicators are being developed from remotely sensed data, for example the Land Surface Temperature (LST), Normalized Difference Vegetation Index (NDVI), Temperature Condition Index (TCI), Enhanced Vegetation Index (EVI), Vegetation Condition Index (VCI), Vegetation Productivity Indicator (VPI) and Water Supply Vegetation Index (WSVI). These satellite derived products together with in-situ data are good indicators for drought assessment (Zhang & Jia, 2013), (Gadisso, 2007). Remote sensing also used to in early drought detection and it's the impact (Zhao et al., 2005).

According to (Berhan et al., 2011) drought monitoring has been done using available meteorological data which is less certain to employing rescue missions and in Ethiopia, there are no significant efforts in calibrating and validating remotely sensed data. High uncertainty of different drought indexes is the result of extrapolation of sparsely distributed meteorological data. Its onset, duration and magnitude can be better determined using remote sensing data (Berhan et al., 2011).

## 2.3. Preciptation

Even though it is not possible to avoid shortage of precipitation, it is possible to predict, monitor and reduce potential adverse effect (Alireza & Josef, 2013). For developing countries like Ethiopia, precipitation is the essential resource since the majority of the population (85%) and the national economy is highly dependent on rain fed agriculture. Distribution in space and time, and total rainfall amount has been seen subject to long term changes in addition to its unpredictability (Dinku et al., 2007). In Ethiopia, the rainfall is a result of different processes. Because of its tropical location rainfall type is mainly convective which makes rainfall spatial distribution high. The probability of orographic rainfall is also very high because of high topography and elevation difference. The amount of precipitation an area receives is the main and important indicator of drought occurrence. If there is reduction in the amount of precipitation, low soil moisture reduction in levels of water bodies will follow (Mirabbasi et al., 2013).

### 2.4. Evapotranspiration

Evapotranspiration is a combination of different processes. It includes evaporation of water from water bodies, soil and intercepted moisture, and transpiration of water from plant's stomata openings (FAO, 2012). Therefore the total amount of water evapotranspired depends on atmospheric forcings like relative humidity, radiation, temperature, clouds and availability of water. Development stage of agricultural crops play a crucial role in determining which component of evapotranspiration is contributing more. As crops grow, the area to be covered by vegetation increases which implies more water is being transpired from plants compared to soil evaporation. Smaller area of the soil will be exposed for available radiation energy to convert the water from liquid state to gaseous state when the vegetation becomes vigorous. High evapotranspiration decreases the soil water available in the crop root zone and consequently, there will be a low yield since the available water cannot fulfil crop water requirement. We differentiate evapotranspiration as follow:

- **Actual evapotranspiration**: is the total amount of water transferred from liquid state to gaseous state from the earth's surface (evaporation) and from plants (transpiration) under actual atmospheric and water condition.
- **Potential Evapotranspiration**: is the amount of water that would evaporate and transpire from earth's surface if there is no water limitation. It measures the demand and, relative humidity, air temperature, surface temperature, wind and radiation play significant role (Gelassie, 2012).
- **Reference Evapotranspiration**: is evapotranspiration from a reference grass which is hypothetical assumed to have 0.12m height, 23% albedo and 70 s/m fixed surface resistance (FAO, 2012).

### 2.5. Normalized difference vegetation index

NDVI is one of the most widely used remote sensing based indicators which has been applied for drought monitoring (Rhee et al., 2010). Spectral reflectance of an object varies from wavelength to wavelength in the solar spectrum. Because of chlorophyll absorption, generally plants have lower reflectance in the red and blue portion of the electromagnetic spectrum. Plants appear green because of higher reflectance in the visible green. Internal cellular structure of plants plays a crucial role in influencing the amount of reflectance. NDVI is obtained using red and NIR channels of the solar spectrum. The change in vegetation reflectance is being used to compute indices which correlate with different plant productivity (Spruce et al., 2011).

The values of NDVI range from -1to 1. Where the minimum positive values indicate bare land, the higher positive values indicate dense vegetation cover, and negative values indicate clouds and water. Since NDVI is a measure of greenness, it gives no information regarding the occurrence of drought. Comparison of time series NDVI values for the same area provides information about the relative health of vegetation and consequently, drought history. But, it varies with temperature, relative humidity and precipitation so that interpreting NDVI values should be spatially dependent (Quiring & Ganesh, 2010).

# 3. DATA AND METHOD

## 3.1. Study area discription

The Amhara region is located in the central and north-west part of Ethiopia. It covers an area of 170,000 km², divided into 11 provinces which contain 105 districts or "Weredas". It accounts 11% of the total area of the country. It is situated from 9° to 13° 45' N and from 36° to 40° 30' E. It shares borders with the Tigray region in the north, Oromia region in the south, Afar region in the east, and Benshangul Gumuz region and Sudan are situated towards the west. Its altitude ranges from about 600 m to 4620 m above sea level. The topography of the region contains highlands, semi-highlands and lowlands. Amhara region is the second largest populous region in the country. Mean annual temperatures of the region are high and have low variability. The annual mean temperature for most of the region ranges from 15⁰C to 21⁰C. But, for some gorge areas, it reaches up to 27⁰C (Gelassie, 2012). The spatial distribution of long term mean annual rainfall varies from 850 mm to 1485 mm. The long term mean annual rainfall of the region is 1165 mm/year. 'Belg' and 'Meher or Kiremt' are the two crop growing seasons when the region receives rainfall from February to June and June to October respectively. 'Meher' takes the lion share from the total annual crop production whereas the remaining small crop production is from the 'Belg' season. Causes of rainfall for the first rainfall season "Belg" in Ethiopia are moisture carrying easterly and south-easterly winds from the Indian Ocean whereas the rainfall in "Kiremt" is because of the ITCZ and convergence in low pressure system which cover many parts of the country (Rosell, 2011). Because of the altitude differences, there is also a contribution from orographic rainfall during both rainy seasons. The main crops that are harvested in Amhara region are Barley, Wheat, Beans, Teff, Sorghum and Maize.

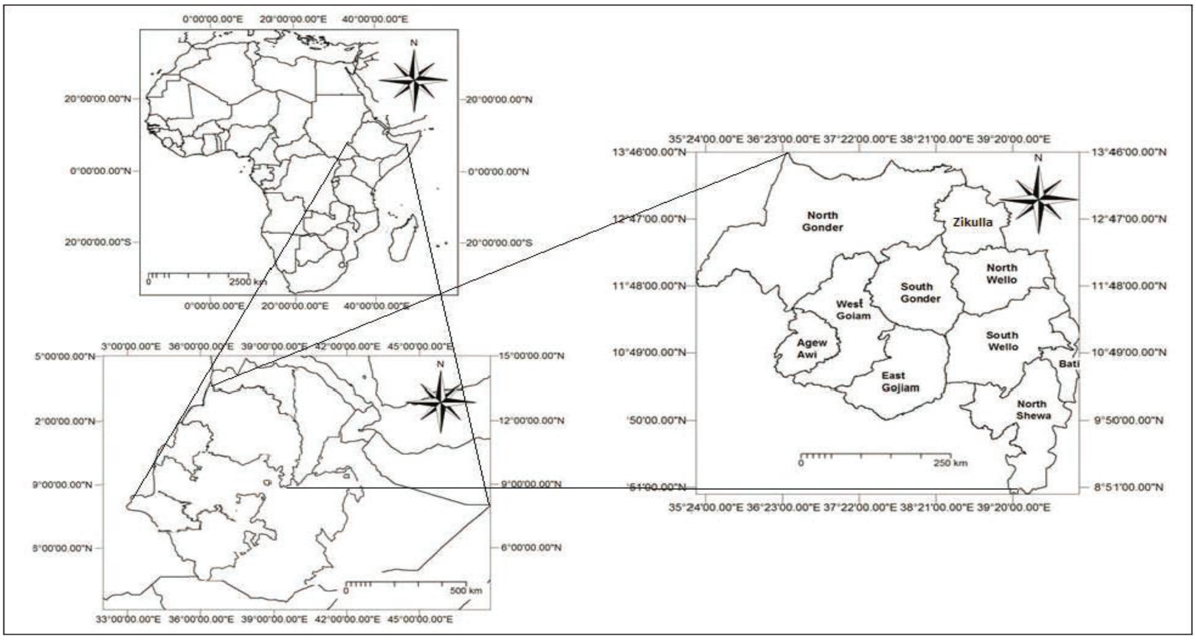


Figure 1 Study Area

## 3.2. Data

### 3.2.1. Remote sensing data

These days, there are many online based environmental data sources which can be accessed to be used for different purposes (Maathuis et al., 2013). According to (Maathuis et al., 2013), the ISOD toolbox is developed to use large amount of free environmental data resources available online. The ISOD toolbox is a plugin toolbox in ILWIS. It uses internet to import data so that it does not need local server. In Situ and Online Data Toolbox version 1.3 is used to download the satellite products used in this study. The picture of the toolbox main menu is given below (figure 2). Details of satellite products, their resolution, methods applied are further described below.

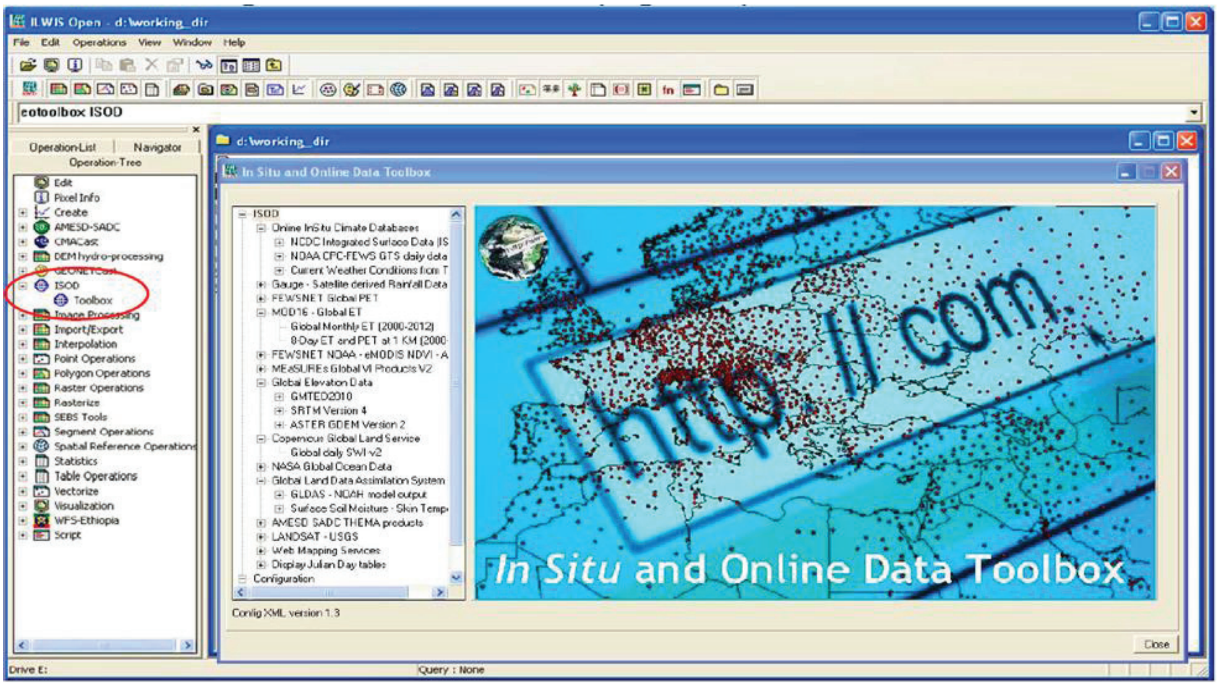


Figure 2 ISOD toolbox

#### 3.2.1.1. Tropical Applications of Meteorology using SATellite (TAMSAT) Rainfall and Climatology

Next to Antarctica, Africa where Ethiopia is located is a continent with lowest density of rain gauges in addition to near complete absence of operational radar installations (Washington et al., 2006) exception to some operational radars in South and West Africa. For water related planning, the main obstacles in Ethiopia are availability, quality and area coverage of in-situ rainfall data (Dinku et al., 2007). Getting quantitative information on real-time rainfall estimates play a crucial role to avoid problems related to excess rainfall and its deficiency. It is of high priority to measure rainfall accurately in Ethiopia. Assimilated rainfall products from model outputs and satellites play a crucial role in filling this gap. Polar orbiting and geostationary satellites provide rainfall estimates using microwave, infrared and visible channels. Polar orbiting satellites monitor emission and scattering of microwaves in clouds and provide better rainfall estimates than geostationary satellites which relate cloud-top temperature to rainfall rate.

TAMSAT estimates are being produced by Reading University in the UK. TAMSAT is a rainfall estimate from Meteosat thermal infrared images and is based on cold convective cloud top temperatures and calibrating these using in-situ rain gauge data (Dinku et al., 2007; Maidment et al., 2012). It provides rainfall estimates for famine and drought prone areas of Africa including Ethiopia (Grimes et al., 1999). TAMSAT product is delivered at 0.0375 degree spatial resolution, at ten day and monthly temporal resolutions. TAMSAT 10 day and monthly rainfall data and anomalies are available from 1983 onwards. Details about the algorithm applied in TAMSAT is well discussed by (Grimes et al., 1999). TAMSAT rainfall climatology is a record of the last 30 years which started from 1983.

#### 3.2.1.2. Moderate Resolution Imaging Spectroradiometer (MODIS) NDVI, ET and PET

Moderate Resolution Imaging Spectroradiometer (MODIS) of National Aeronautics and Space Administration's (NASA) has improved atmospheric corrections, higher spectral and spatial resolutions, and more precise geo-location than National Oceanic and Atmospheric Administration's (NOAA) Advanced Very High Resolution Radiometer (AVHRR). Due to the challenges users faced to use for real time application in relation to mosaicking, reprojection, subsetting and format conversion of NASA-EOS MODIS products, U.S Geological Survey's (USGS) Earth Resources Observation and Science (EROS) centre started to generate enhanced MODIS products based on NASA's Earth Observing System (EOS) MODIS data. MODIS's frequent repeat cycle and higher spatial resolution (250 m) compared to AVHRR enable it to be used more widely in vegetation studies (Brown et al., 2008). MODIS is a 36 band sensor onboard Terra and Aqua satellites which overpass morning (10:30) and afternoon (13:30) local time respectively. eMODIS NDVI data is available since 2001-2013, composited in seven day intervals.

MOD16 ET and PET are calculated using inputs (leaf area index (LAI), albedo, Enhanced Vegetation Index (EVI), Land cover) from MODIS satellite and NASA's Global Modelling and Assimilation Office (GMAO) daily meteorological reanalysis data set. It uses the algorithm by (Mu et al., 2007) as reference and latter (Mu et al., 2011) improved it. MODIS ET and PET datasets are available from 2000 to 2012 with one $Km^2$ spatial resolution in mm/8days. Eventhough monthly and yearly temporal scales are available, the 8 days temporal products are used here.

#### 3.2.1.3. United States Agency for International Development (USAID) Famine Early Warning System Network (FEWSNET) Rainfall, climatology and PET

Rainfall estimates of FEWSNET are produced by the Climate Prediction Centre of NOAA. Cloud top temperature (235K) and rainfall data from gauge stations are being used in this estimation (http://earlywarning.usgs.gov/fews/africa/web/readme.php?symbol=dailyrfe) continuing from RFE 1.0. The Advanced Microwave Sounding Unit (AMSU) and Special Sensor Microwave/Imager (SSM/I) onboard of the Defence Meteorological Satellite Program satellites are new rainfall estimating instruments used in RFE 2.0 (Climate Prediction Center, 2006). The data is available from 2000 onwards with spatial resolution of 0.1 degree. The data is available daily and ten day estimates, and spatially, it covers the

African continent. Ping-Ping Xie's algorithm is applied for RFE 2.0. Details can be found in (Xie & Arkin, 1996). ARC2 is the rainfall climatology using RFE data records from 1983 until 2011.

NOAAS's GDAS climate parameter data (wind speed, solar radiation (short wave, long wave, incoming and outgoing), atmospheric pressure, and temperature of the air) are used to calculate potential evapotranspiration (http://earlywarning.cr.usgs.gov/fews/global/web/readme.php?symbol=pt). Daily PET will be obtained by summing PET computed every six hours. FEWSNET PET is calculated by adopting Penman-Monteith evapotranspiration for reference crop evapotranspiration. Spatially, it covers the whole globe with one degree resolution daily.

| | eMODIS NDVI | FEWSNET PET | TAMSAT rainfall | MOD16 ET & PET | TAMSAT Rainfall climatology | ARC2 RF climatology | FEWSNET RFE |
|---|---|---|---|---|---|---|---|
| Temporal resolution | Dekadal | Daily | Dekadal | 8 days | Dekadal | Dekadal | Dekadal |
| Spatial resolution | 250 m | $1^0$ x $1^0$ | $0.0375^0$ x $0.0375^0$ | 1 km X 1 km | $0.0375^0$ x $0.0375^0$ | $0.1^0$ X $0.1^0$ | $0.1^0$ X $0.1^0$ |
| Availability in time | 2002-2012 | 2002-2012 | 2000-2012 | 2000-2012 | 1983-present | 1983-2011 | 2002-2012 |
| Download and pre-processing | ISOD | ISOD | ISOD | ISOD | ISOD | ISOD | ISOD |

Table 1 Remote sensing derived products

### 3.2.2. In-situ data

Precipitation and temperature data are collected for 18 principal stations from national and regional meteorological agency offices. Based on availability of recorded data for 30 years and full functioning gauges, only 11 stations are selected to be used in this study. These 11 stations have recorded data from 1982 to 2012. Because of the data sharing policy of NMA of Ethiopia, the data obtained are on monthly basis. Informal interview of randomly selected farmers is carried out. Random physical observation to see the actual condition of land cover and taking photos have also been carried out. Thirteen ground control points were collected using GPS at different locations in the study area. It should be noted that the physical observations and control points collected are very limited compared to the area of the Amhara region.

| | Name | Latitude (degree) | Longitude (degree) | Elevation (m) |
|---|---|---|---|---|
| 1. | Ayehu | 10.45 | 36.55 | 1725 |
| 2. | Bahir Dar | 11.36 | 37.24 | 1770 |
| 3. | Chagni | 10.57 | 36.30 | 1620 |
| 4. | Debre Markos | 10.20 | 37.40 | 2515 |
| 5. | Debre Work | 10.44 | 38.08 | 2740 |
| 6. | Gonder | 12.33 | 37.25 | 1967 |
| 7. | Debre Tabor | 12.10 | 38.02 | 2690 |
| 8. | Debre Birhan | 9.60 | 39.50 | 2750 |
| 9. | Aykel | 12.32 | 37.03 | 2150 |
| 10. | Combolcha | 11.07 | 39.44 | 1903 |
| 11. | Motta | 11.05 | 37.52 | 2440 |

Table 2 Location and Elevation of Meteorological Stations

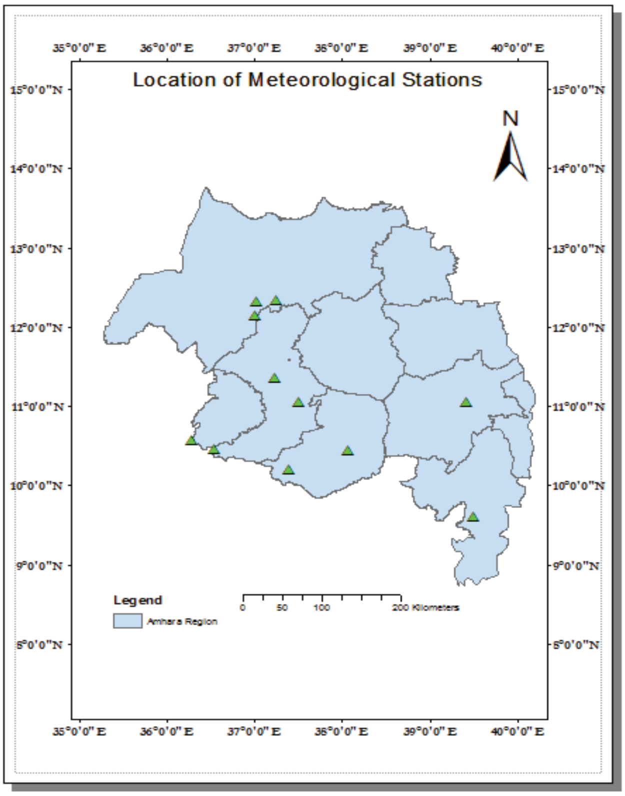


Figure 3 Location of Meteorological Stations

### 3.2.3. Ancillary data

The land cover map of the Amhara region is extracted from the ESA Global Land Cover map of 2009 developed in collaboration with EEA (European Environment Agency), JRC (Joint Research Centre), UNEP (United Nations Environment Program), GOFC ( Global Observation of Forest Cover), IGBP (International Geosphere-Biosphere Program) and FAO (Food and Agriculture Organization of United Nations). The data is freely available from http://due.esrin.esa.int/globcover/. Because of its good spatial resolution (300 meter) and matching well with recognized land cover classes (water bodies and rainfed crop lands, this land cover map is selected. Originally, the region had 12 land cover classes which are reclassified into nine classes by merging available forest types of the region. The actual land cover coincides with known land cover classes of the region. The physical observations and the number of control points collected are very limited in verifying the quality of the land cover map of the study area.

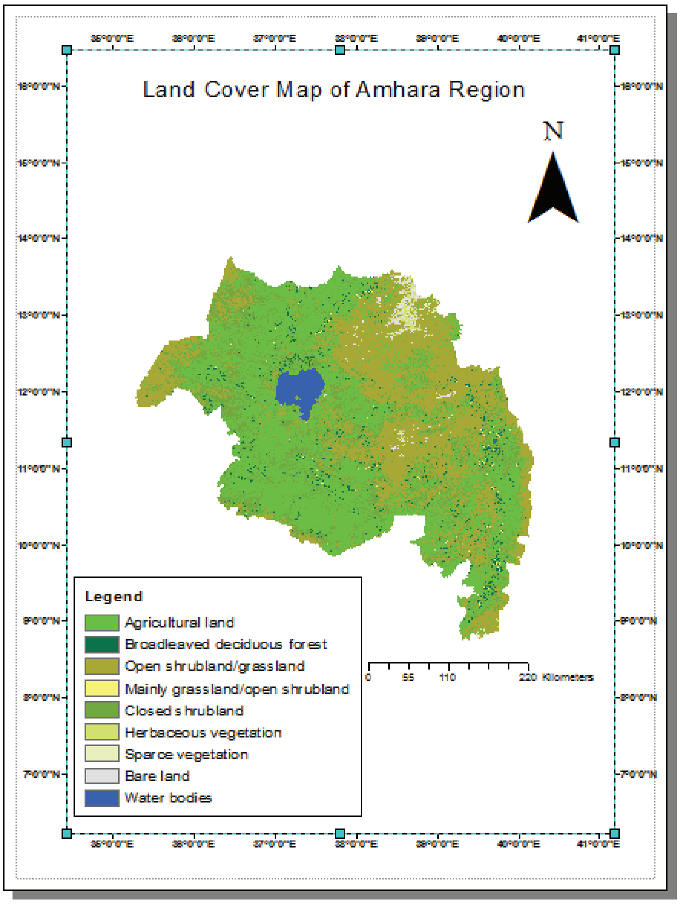


Figure 4 Land cover map of Amhara region

## 3.3. Method

### 3.3.1. Farmers Interview

Five groups of people whose farmlands are located nearby are interviewed informally. The farmers are randomly selected and the groups included both genders. The questions asked include identifying the years at which they experienced drought and for what reason according to them the drought happened. The farmers were also asked about the frequency of drought occurrence.

### 3.3.2. Rainfall reliability check for gauge stations

Pre-processing of in-situ rainfall and temperature data included manual checking to make sure unreliable records are not included, identification of missing data, and verification of station location. After looking at all 18 stations, 11 of them which are most complete are selected. Average values are used to fill some of the missing data.

In order to make sure that the rainfall measured from gauge stations is representing the reality, checking other potential effects on the gauges observation is important. Moving gauges from place to place can affect their consistency. Double-mass curve analysis is applied to assure that the gauge measurements are free from potential effects. Their exposure can also be affected due to changes within their surroundings. Double-mass curve assumes that the value of each gauge station against the mean value of all stations during the same period of time plots as a straight line if the data are proportional. If the values of gauge stations and their mean value have good correlation, it implies that the stations represent the reality.

### 3.3.3. Comparison and Validation of Satellite Products and In-situ Data

#### 3.3.3.1. Pre-processing and general methodology

Statistical approach is used after relevant pre-processing of data. Average values are used to fill missing values. Monthly mean values for in-situ rainfall and temperature data are calculated. Average and sum functions of ILWIS are used to calculate statistics of all satellite products when necessary.

Inverse distance weighted (IDW) is an interpolation technique used to convert station based meteorological point data to area to see the spatial rainfall climatology of the region. It is commonly used for point data, and works based on the principle that the areas closer to the station should weight more than areas far from the station (Abraha, 2013). After in-situ precipitation data is pre-processed, pixel to pixel and point to pixel comparison is applied to find the correlation coefficient between satellite products and satellite products and in-situ data. Root mean square error is calculated to see the difference between two data sets.

#### 3.3.3.2. Validation and Comparison of Satellite rainfall products using in-situ data

Dekadal TAMSAT rainfall of 30 years is obtained using the ISOD Toolbox and is used for all years under consideration. The first validation of TAMSAT estimated rainfall is conducted using average monthly rainfall of 30 years with the assumption that longer data records provide higher accurate information about the capability of satellite product in reproducing gauge data by reducing the effect of uncertainties. Actual monthly TAMSAT RFE of 2010 is also validated using in-situ rainfall of the same year. Here, the validation method applied is point to pixel to avoid the problems of interpolation that would appear if pixel to pixel method was used. The comparison between ARC2 rainfall climatology and TAMSAT rainfall climatology is done after resampling TAMSAT to 0.1 degree spatial resolution of ARC2. These two products are compared pixel to pixel. The method applied is graphically represented in the following figure.

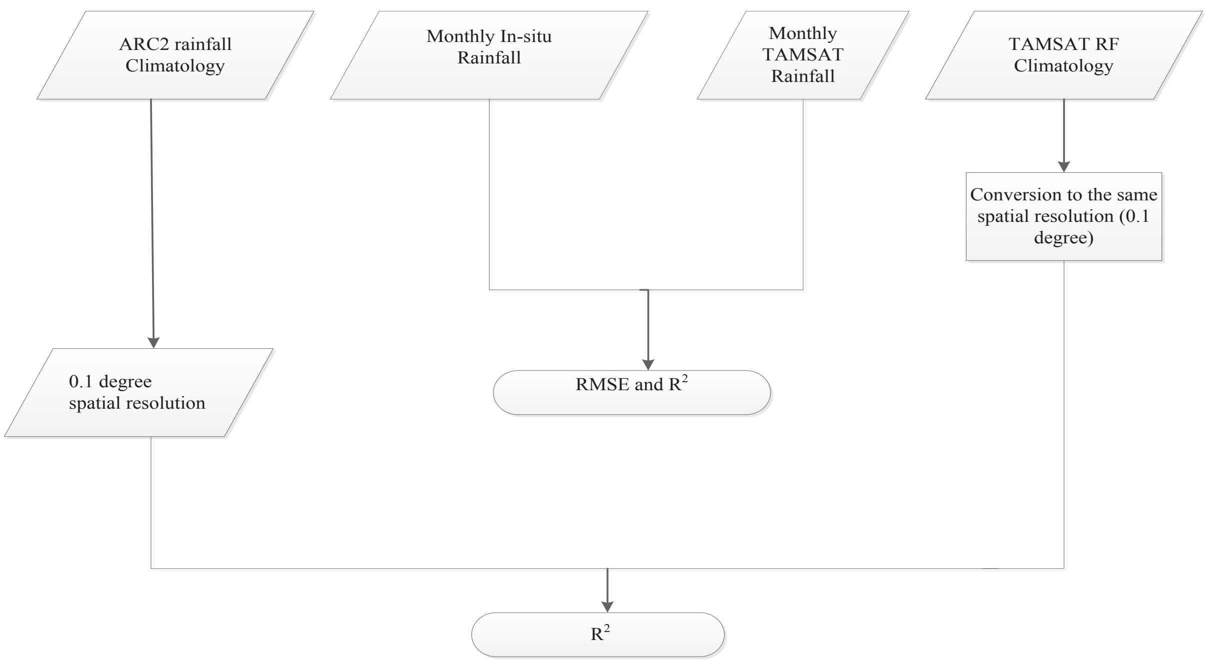


Figure 5 Validation and Comparison of satellite derived rainfall and in-situ rainfall data

#### 3.3.3.3. Comparison of Satellite Potential Evapotranspiration Products and Reference Evapotranspiration

Availability and quality of data is most common constraint for water related research in developing countries (Enku & Melesse, 2013). This problem appears also for the Amhara region therefore a method which is less data intensive has to be adopted. The method selected to calculate reference evapotranspiration is recently developed and maximum temperature dependent, and called the "Enku Method"

$$ET_o = \frac{(T_{\max})^n}{k}$$

Where; ETo is the reference evapotranspiration in mm/day. Even though it can be calibrated for local conditions, n = 2.5 is directly used in this study. Coefficient k can also be calibrated for local conditions. K ranges from 600 for lower mean annual maximum temperature areas to 1300 for higher mean annual maximum temperature areas. The coefficient k can also be approximated using the following equations; for the study area, the seasons are either dry (October-April) or wet (June-September). For this reason, the coefficient k is approximated using k=73*Tmm_1015 for dry seasons, and k=38*Tmm_63 for wet seasons. $T_{mm}$ ($^{o}$C) is the long term daily mean maximum temperature for the season under consideration.

Reference ETo is calculated for 30 years using monthly temperature data. Calculated monthly ETo for 10 years (2002 – 2011) is compared with Monthly PET obtained from FEWSNET and MOD16 (from 2002-2011). Comparison is done for ten years data for which the data are available for both satellite products as well as calculated reference evapotranspiration. The method applied is point to pixel comparison. MOD16 PET and FEWSNET PET are compared twice. First, they are compared pixel to pixel using their actual resolution and the second comparison is after MOD16 is aggregated to 1 degree spatial resolution of FEWSNET PET. The method used in comparison of satellite PET products and calculated reference ETo is described in the figure below.

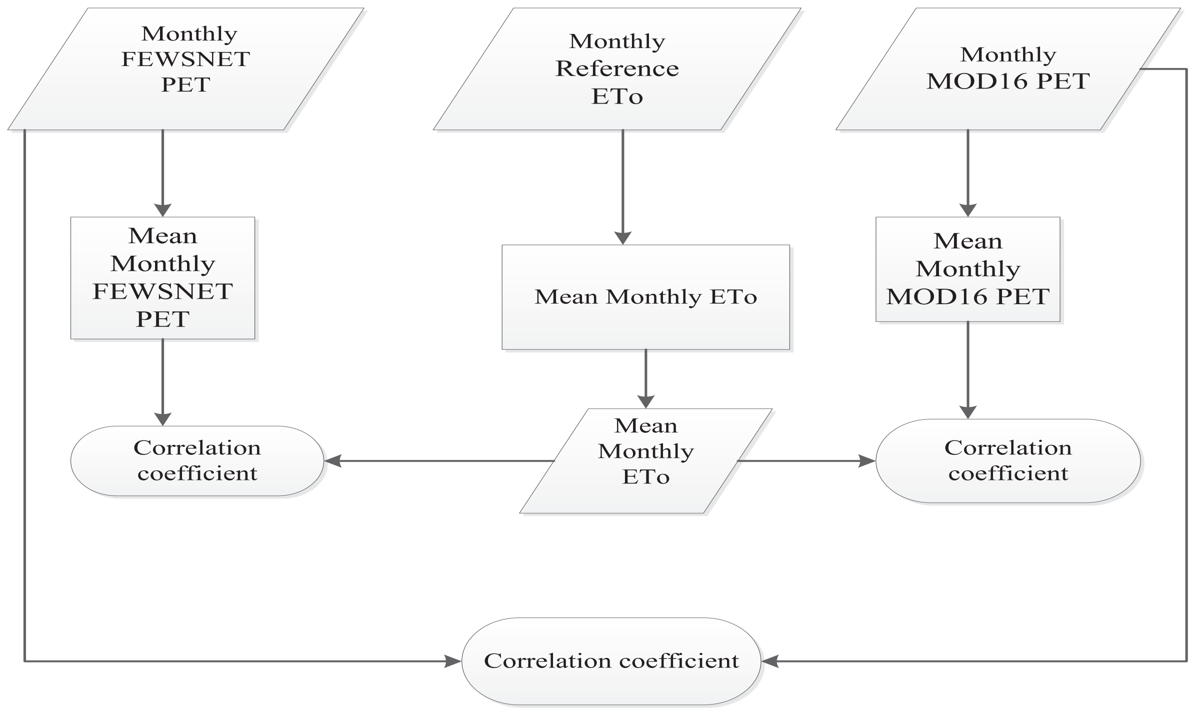


Figure 6 Reference Evapotranspiration, MOD16 PET and FEWSNET PET flowchart

#### 3.3.4. Temporal Drought Assessment

Temporal drought assessment is done using FEWSNET PET and RFE, MOD16 ET and PET, TAMSAT RFE, and eMODIS NDVI satellite products. SPIRITS is used in order to see the temporal trend of drought using selected indicators.

#### 3.3.5. Software for the Processing and Interpretation of Remotely Sensed Image Time Series (SPIRITS)

Software for the Processing and Interpretation of Remotely Sensed Image Time Series (SPIRITS) is mainly designed to analyse time series of low and medium resolution sensors (e.g. NOAA-AVHRR, MSG-SEVIRI, TERRA/AQUA MODIS, METOP-AVHRR, and SPOT-VEGETATION) datasets and rainfall products derived from satellites (https://rs.vito.be/africa/en/software/Pages/Spirits.aspx). SPIRITS is used to extract statistics (mean, maximum, absolute difference average, minimum and others) of inputs by overlying with land cover classes and/or administrative regions (provinces or districts) (Herman & Dominique, 2013). According to (Herman & Dominique, 2013), extracting statistics of input data can be done using different methods based on land use/land cover information. These are; regional unmixed means if there is no information available regarding land use/land cover of an area, hard classification if every pixel is 100% within a certain land cover class, and classification by using area fraction of inputs. The method applied in this study is hard classification method.

#### 3.3.5.1. Pre-processing of Data for SPIRITS

All the remote sensing data used in this study are downloaded using ILWIS batch routines. Conversion of temporal scale, defining mapping extent of satellite products, creating new geo-reference, and resampling (nearest neighbour and bicubic from high to low resolution and from low to higher resolution respectively) have also been carried out when necessary. Maplists in ILWIS have been created for data that is downloaded on a daily basis and subsequently aggregated to get dekadal time steps.

#### 3.3.5.2. Time Series Converter Tool

Pre-processing of time series data is tedious and it takes a lot of time (Maathuis & Schouwenburg, 2013). SPIRITS uses specific naming conventions and all the files have to be in ENVI raster format with additional information in the header file. All the images should have their header file and data in the same directory. Even though renaming and importing are possible in SPIRITS, in order to make this pre-processing easy, the TS converter tool (Maathuis & Schouwenburg, 2013) is used otherwise it would take a longer time to finish. All the maplists created are renamed and exported using the TS converter tool. Extracting Region of Interest (ROI), creating quick look map templates for all satellite products and masking was performed. Shapefile of administrative sub-regions of Amhara region and land cover map (see section 3.2.3) are used as additional inputs so that all the statistics are extracted for each administrative region and for each land cover type. Hard classification method is extracting regional unmixed mean (RUM) statistics for an administrative area considering each land cover type separately. Figure 7 below shows the work flow used for extraction of statistics and visualizing of the results is presented.

MOD16 ET and PET products analysed using the method below are eight day composite data. Because of the naming conventions implemented in SPIRITS, a time series data should be daily, dekade, monthly, and/or yearly. But, for MOD16 PET and ET, the highest temporal resolution of these data is eight day. SPIRITS only accepts 36 dekads in a year. Therefore, in order to analyse these products in dekades, the second eight days (9, 49, 89, 129, 169, 209, 249,289 329 and 361) of months in all years are omitted.

Eventhough FEWSNET RFE data is available since 2000, after examining the data for all years, the first two years are not considered because of abnormal high precipitation values. Therefore, 2000 and 2001 are neglected. eMODIS NDVI data downloaded and analysed in this study is only retrieved for the growing seasons (June –October).

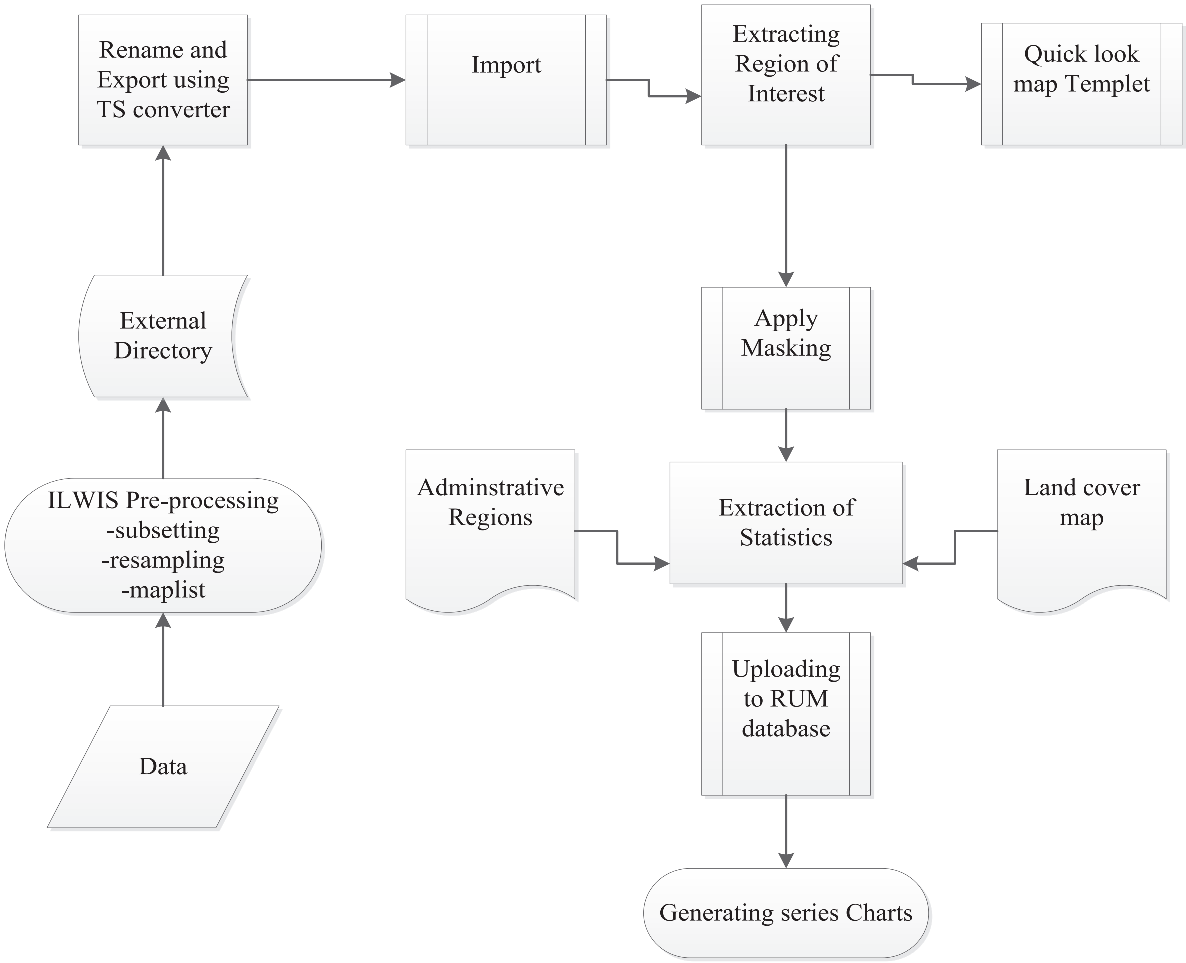


Figure 7 Extracting statistics using SPIRITS

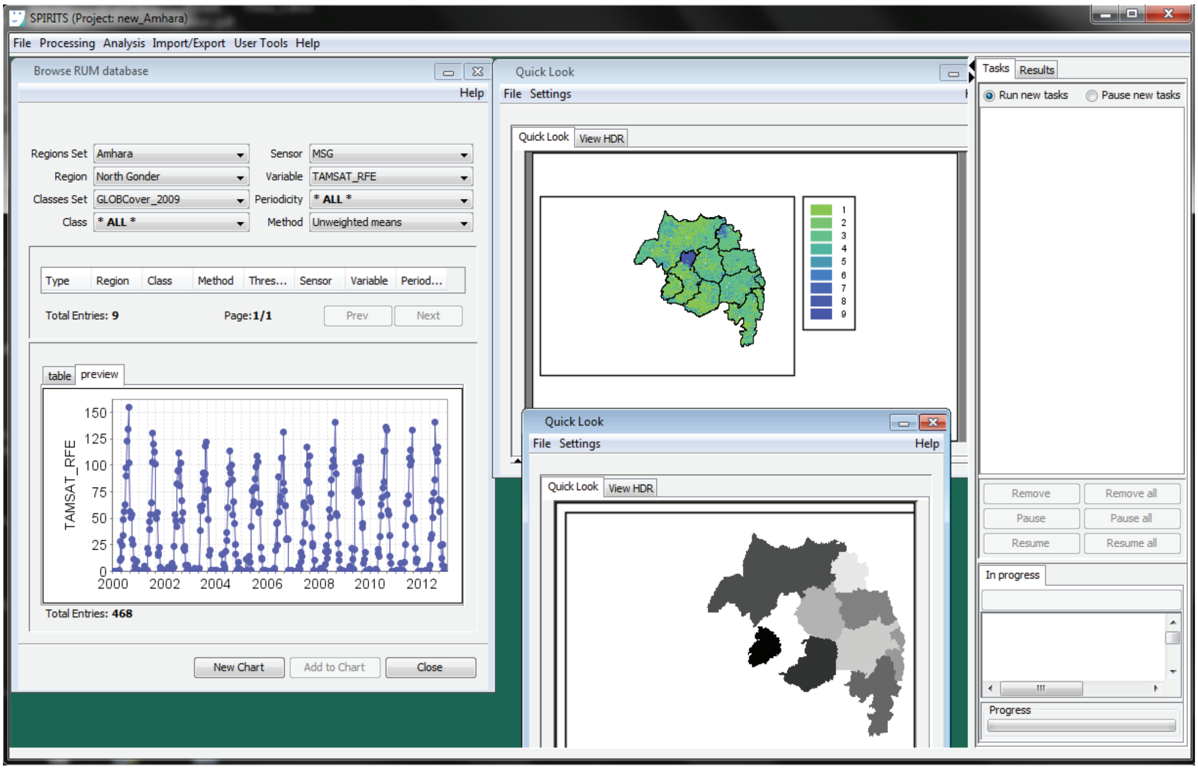

Figure 8 SPIRITS working window

# 4. RESULT AND DISCUSSION

## 4.1. Farmers interview

Randomly selected farmers are interviewed about their experience of drought in the years passed. The farmers replied that agricultural yield obtained was more related with the agricultural practices such as ploughing, weeding and mainly the application of fertilizer. They could not indicate and relate the amount and distribution of rainfall of a year with the yield obtained in that specific year. This might be because of their illiteracy and difficulty in assessing the rainfall amount and pattern of years passed.

## 4.2. Reliability check of rainfall data for gauge stations

Double-Mass Curve analysis is applied to make sure the location, observation and exposure do not affect the rainfall recorded by the stations. All eleven stations are free from these effects and therefore changes observed in the following analysis of in-situ data are result of meteorological changes. All the gauges showed a good correlation coefficient. The minimum and maximum values of RMSE are found at Motta and Chagni stations respectively. The scatter plots showing the relationship and correlation coefficients are available in appendix A.

| | Name | Correlation Coefficients ($R^2$) | RMSE (mm) |
|---|---|---|---|
| 1. | Ayehu | 0.8451 | 41 |
| 9. | Aykel | 0.9655 | 20 |
| 2. | Bahir Dar | 0.992 | 41 |
| 3. | Chagni | 0.9096 | 50 |
| 10. | Combolcha | 0.9021 | 36 |
| 8. | Debre Birhan | 0.8739 | 44 |
| 4. | Debre Markos | 0.9702 | 21 |
| 7. | Debre Tabor | 0.9885 | 46 |
| 5. | Debre Work | 0.9714 | 40 |
| 6. | Gonder | 0.9726 | 19 |
| 11. | Motta | 0.9813 | 15 |

Table 3 Reliability check for gauge stations

The 30 years of rainfall data obtained from NMA Ethiopia is used and the IDW interpolation technique is applied to produce the rainfall climatology for Amhara region (figure 9). The spatial distribution of in-situ rainfall indicates that the eastern part of the Amhara region receives less rainfall. Spatial variability of rainfall in the region is high (Bewket & Conway, 2007). The eastern part of Amhara region shares the border with the Rift valley. Because of close proximity to the edge of the Rift easterly winds from the Indian Ocean do not cause high rainfall over the Combolcha and Debre Birhan stations. Also low rainfall at Debre Work station is recorded because of its location in the valley. Figure 10 shows the monthly rainfall climatology of 11 stations (in millimetre). It is used to assess the rainy season and agricultural growing season (NDVI) based on which comparison and validation of rainfall satellite products is done.

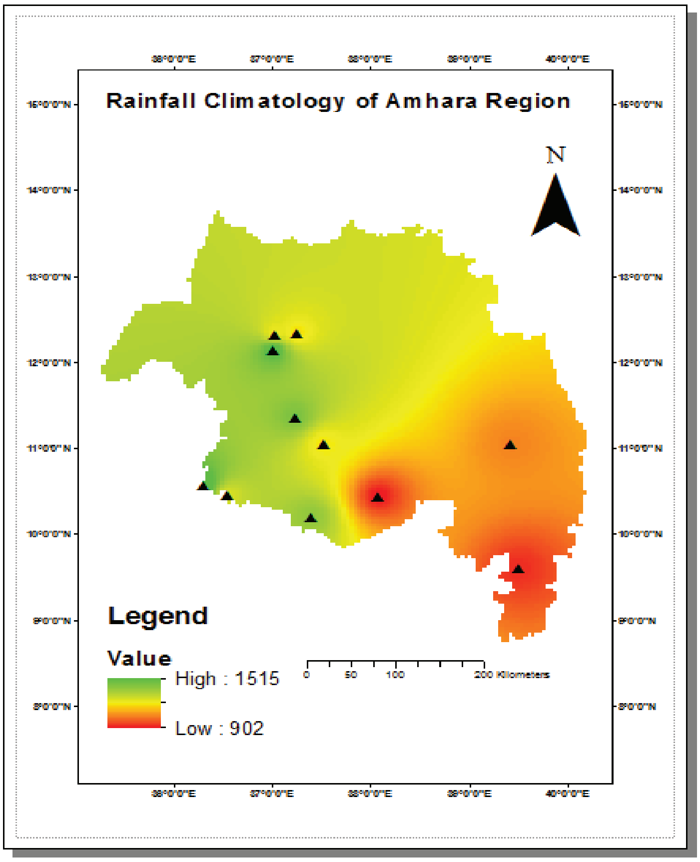


Figure 9 Spatial rainfall climatology of Amhara region

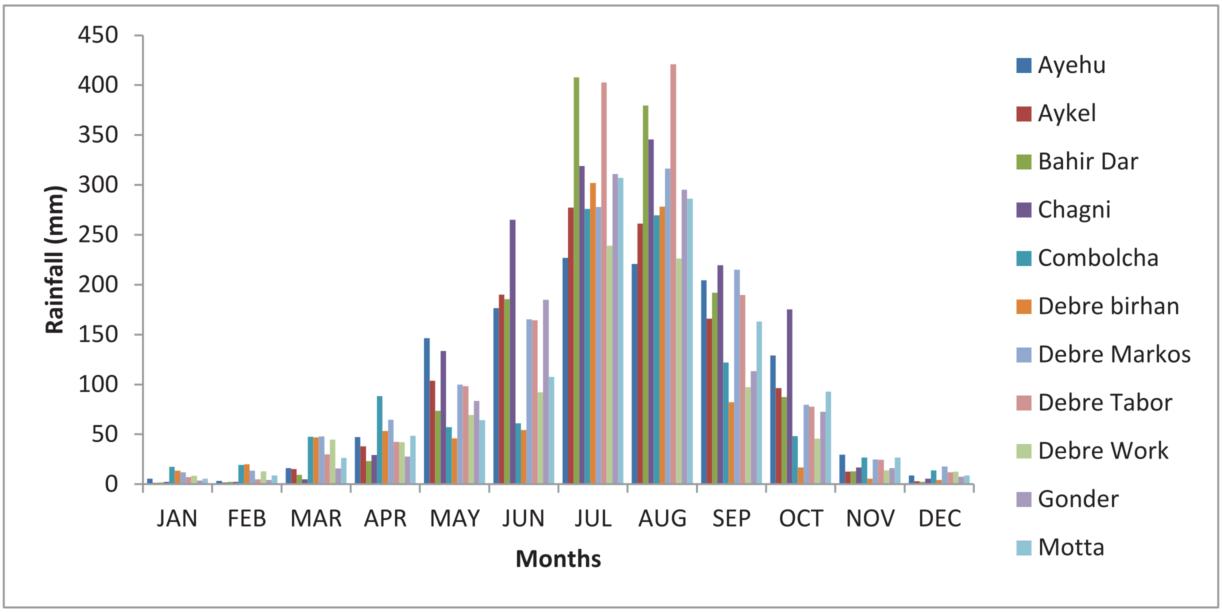


Figure 10 Monthly rainfall climatology of 11 stations

## 4.3. Comparison and validation of satellite products using In-situ data

### 4.3.1. Comparison and validation of rainfall products

Validation of TAMSAT rainfall product is done twice. The first validation is done using averaged monthly (May to October) rainfall data of 30 years for both gauges and pixel values where the gauges are located (figure 11). The point to pixel validation of TAMSAT rainfall using the gauge rainfall and values of pixels where the stations located shows high correlation coefficient ($R^2$=0.93). The correlation coefficient indicates they have direct relationship. Except in September, TAMSAT satellite product under estimated rainfall. Other studies conducted over the region which used different stations reported $R^2$=0.75 (Dinku et al., 2007).

The second validation is carried out using monthly rainfall of the year 2010 to reduce the uncertainties in both in-situ rainfall data and TAMSAT rainfall estimate. The year 2010 is selected because the data obtained from all the gauges are complete. This validation of TAMSAT rainfall estimate is carried out for each station. The RMSE shows that there is high difference between TAMSAT RFE and gauges rainfall at Debre Birhan and Debre Tabor whereas the minimum difference between these two data sets is observed at Combolcha station. The correlation coefficient and RMSE of all stations are presented in table 4 below. Pixel to pixel validation of TAMSAT with interpolation in-situ rainfall data would be biased towards the interpolation method used. Therefore, only point to pixel validation is applied.

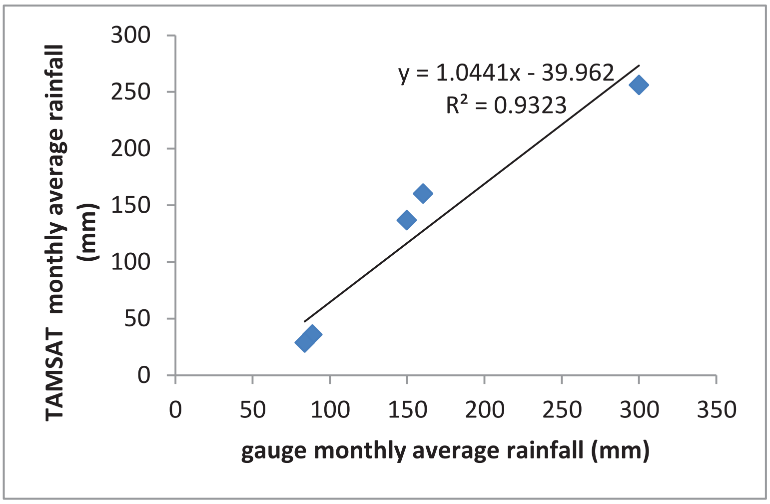


Figure 11 Validation of TAMSAT rainfall using gauge data

| | Name | Correlation Coefficients ($R^2$) | RMSE (mm) |
|---|---|---|---|
| 1. | Ayehu | 0.76 | 47 |
| 9. | Aykel | 0.79 | 51 |
| 2. | Bahir Dar | 0.92 | 63 |
| 3. | Chagni | 0.78 | 72 |
| 10. | Combolcha | 0.76 | 39 |
| 8. | Debre Birhan | 0.38 | 87 |
| 4. | Debre Markos | 0.78 | 60 |
| 7. | Debre Tabor | 0.90 | 87 |
| 5. | Debre Work | 0.69 | 55 |
| 6. | Gonder | 0.77 | 53 |
| 11. | Motta | 0.84 | 75 |

Table 4 TAMSAT monthly rainfall validation using in-situ rainfall for 2010

#### 4.3.2. Comparison of Africa Rainfall Climatology Version 2 (ARC2) and TAMSAT Rainfall Climatology products

Pixel to pixel comparison is conducted between ARC2 and TAMSAT rainfall climatology products (figure 12) by aggregating TAMSAT 0.0375 degree resolution to 0.1 degree spatial resolution of ARC2. A very good correlation coefficient of R=0.98 is obtained. The relationship between them is strong and shows that when the TAMSAT rainfall climatology increases, ARC2 rainfall climatology increases. Both products are good in estimating low rainfall amounts. It is reported that ARC2 underestimates rainfall in areas where GTS gauge daily reports are not available and orographic rainfall can occur (Novella & Thiaw, 2013).

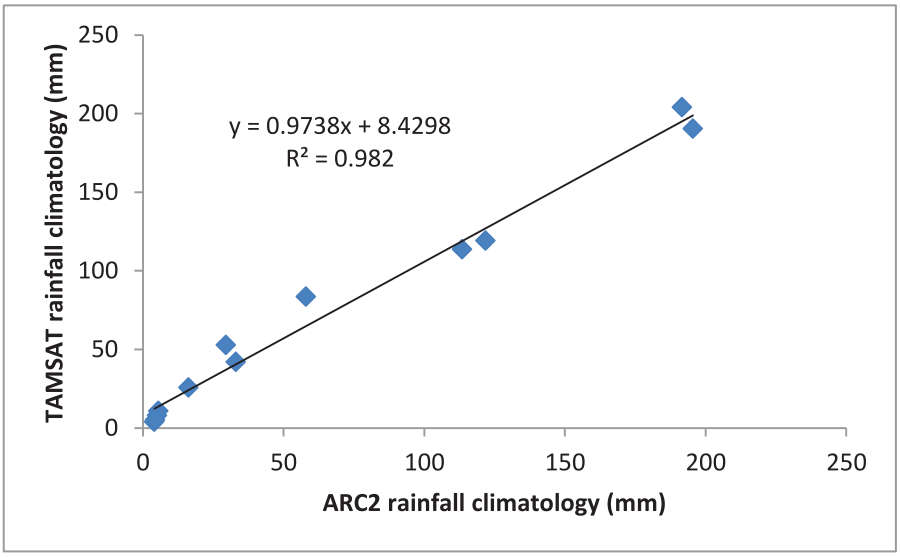


Figure 12 Comparison between TAMSAT rainfall climatology and ARC2 rainfall climatology

### 4.3.3. Comparison and Validation of Satellite derived PET products using Enku's Reference Potential Evapotranspiration Method

#### 4.3.3.1. Estimation of Reference Potential Evapotranspiration Using Enku Method

Monthly average of 30 years reference evapotranspiration is calculated using Enku's simple temperature method (figure 13). Enku's method has been validated using different developed evapotranspiration estimation methods (Enku & Melesse, 2013). Six of the meteorological stations selected for this study were used for these comparisons. According to (Enku & Melesse, 2013), the comparison result against the most popular Penman Monthiez method, Hargreaves (HAR) method which uses temperature and Piche evaporimeter, showed that this method performs good. The correlation coefficient ($R^2$) found against these three methods is 0.74, 0.91 and 0.75 respectively. It has also been validated with HAR method over wet and dry seasons, and $R^2$ found is 0.82 and 0.84 respectively (Enku & Melesse, 2013).

According to the result obtained, most of the stations (10) have low ETo during the rainy season (from May to end of September). This is because of the evaporative demand of the atmosphere is largely fulfilled by the rainfall. The amount of water vapour available in the air during the summer season is lower than during winter season. During summer, the amount of water that would evaporate from different sources and transpire from plants increases. Low temperature of the area during winter season (Kiremt) contributes to low ETo. Since the method applied is totally temperature dependent, the amount of calculated ETo is lower during the winter season. But, for areas which have high temperature and low rainfall amount during winter like Combolcha station, it is different.

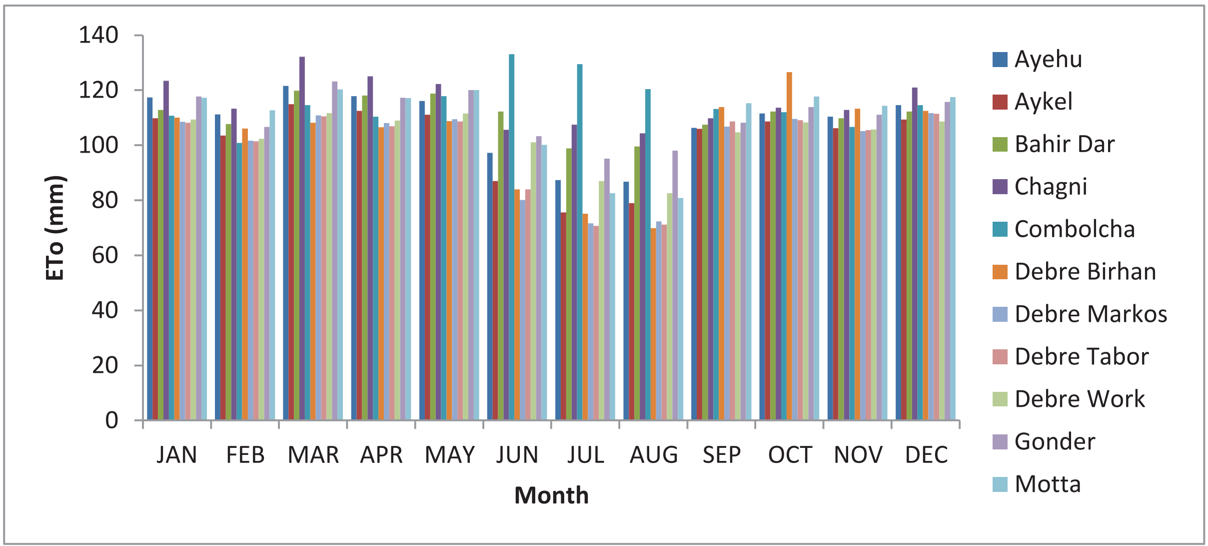


Figure 13 Average reference evapotranspiration calculated using Enku's method

#### 4.3.4. Comparison of potential Evapotranspiration satellite products and Enku method

Reference evapotranspiration calculated using Enku's method is compared against MOD16 and FEWSNET PET satellite products. The comparison is conducted using point to pixel method. The comparison made against FEWSNET PET and Enku's ETo shows a correlation coefficient of $R^2$= 0.72 (figure 14 (a)). MOD16 PET is also compared against Enku's ETo (figure 14 (b)) and shows a correlation coefficient of $R^2$= 0.74. The comparison between Enku's ETo and MOD16 PET shows a slightly higher correlation coefficient because of a better spatial resolutions of the MOD16 PET satellite product. Calculated reference evapotranspiration using Enku's method has a direct and strong relationship with both satellite PET products. Both satellite products give higher estimates.

Pixel to pixel inter-comparison is also done between PET satellite products (MOD16 and FEWSNET PET) figure 14 (c). The comparison obtained between MOD16 PET and FEWSNET PET shows a correlation coefficient of $R^2$= 0.83. In order to examine if low spatial resolution of FEWSNET PET affects the correlation coefficient, MOD16 PET is aggregated to one degree spatial resolution of FEWSNET PET. After MOD16 PET is resampled using nearest neighbour technique to one degree, the correlation coefficient improved from 0.83 to 0.84 (figure 14 (d)). In both cases, the relationship between PET satellite products is direct and strong. Because of the differences in data sources in estimating PET, (FEWSNET uses NOAA's GDAS climate parameter data whereas MOD16 uses NASA's Global Modelling and Assimilation Office (GMAO) meteorological data and MODIS satellite land cover information) the values estimated using MOD16 PET are substantially higher compared to the FEWSNET PET. The difference in spatial resolution can have contribution.

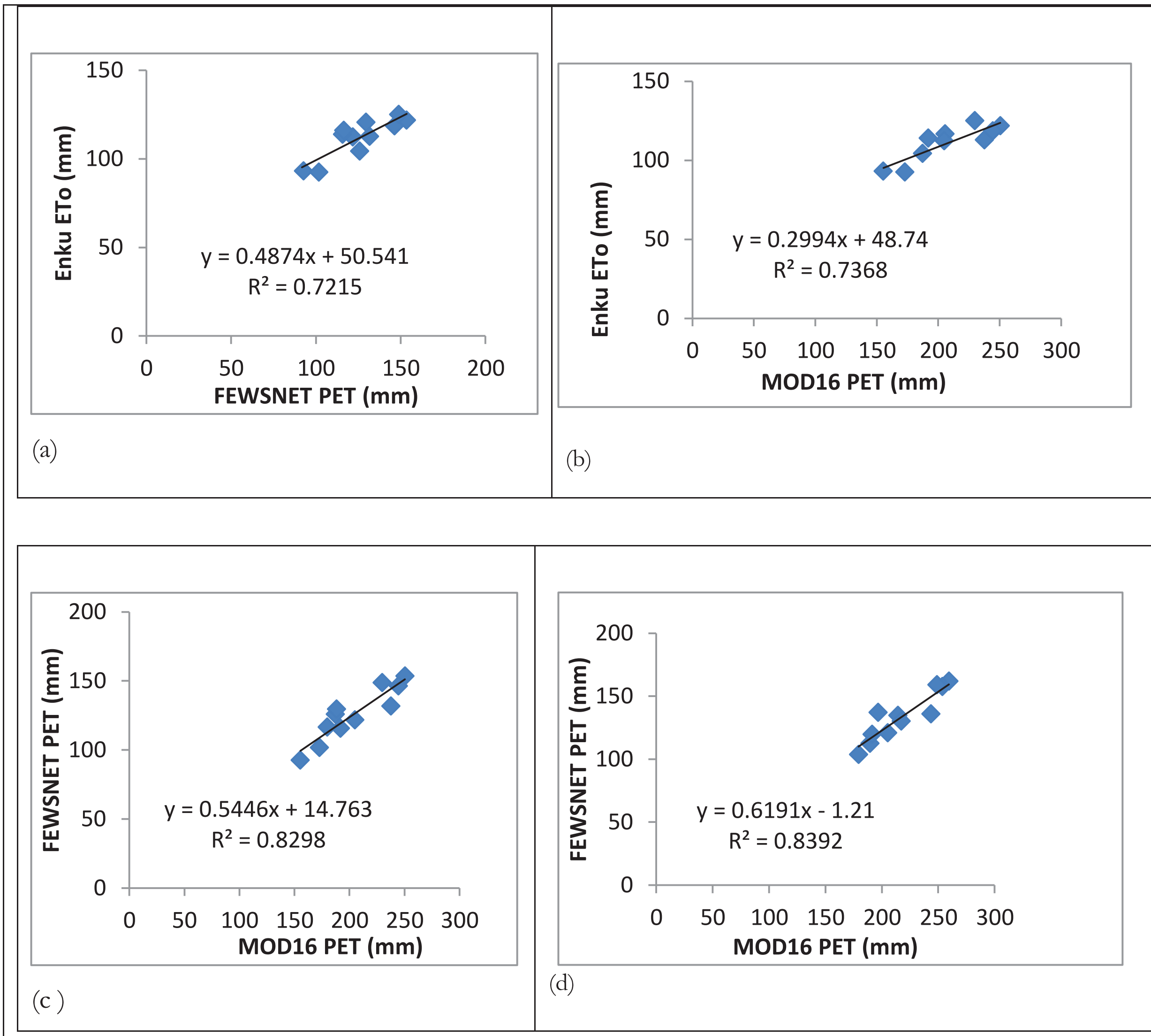


Figure 14 (a) Comparison of FEWSNET PET and Enku ETo, (b) comparison of MOD16 and Enku's ETo, (c ) comparison between FEWSNET PET and MOD16 PET before aggregation, (d) comparison between FEWSNET PET and MOD16 PET after MOD16 PET is aggregated, and outliers are removed

Figure 14 show that the inter-comparisons between PET from different sources show direct relationship and reasonable correlation coefficients. According to figure 14 a and b, calculated reference ETo using Enku's method underestimates when compared to the satellite products. The approximations made for coefficient k (based on season) in calculating Enku's ETo can also contribute for the difference in ETo values obtained. The relatively low correlation coefficient between FEWSNET PET and Enku's ETo shows that there is spatial variability of ETo over the Amhara region. This is because of large elevation and topographical variations (elevation ranges from 600 m to 4620 m above sea level) in the area within relatively short distances and these are not appropriately captured by the 1 degree resolution of the FEWSNET PET product.

### 4.4. Temporal drought trend assessment using SPIRITS

The data is analysed for all administrative sub-regions of the Amhara region. In order to select administrative sub-regions to include in this analysis, agricultural yield, area coverage, experience of drought and population size from census conducted by CSA of Ethiopia in 2007 are used as criteria. Based on this information, North Gonder fulfils many of these criteria. It is the sub-region with (45,945 square kilometres) with the largest population (2,929,628) and high agricultural yield. Even though the land cover map of the Amhara region has 9 classes, the results discussed below refer only to agricultural land cover. In order to see the variations, extracted statistics using a similar methodology for North Shewa, which has different climatology, are included in the appendix.

Definition of statistical parameters calculated using SPIRITS. According to (Herman & Dominique, 2013), the statistics calculated in section 4.4 are defined as follows:

**Normal:** is the actual value of an indicator for a specific dekade.

**Minima:** is the minimum value of an indicator over all the years; "Min(X(y,P)) over all years y".

**Maxima:** is the maximum value of an indicator over all the years; "Max(X(y,P)) over all years y".

**Average:** is the sum of values of a dekade in all years divided by the number of dekades; "Sum(X(y,P)) /Count(X(y,P)) over all years y".

**Absolute difference average:** is the value obtained by subtracting the average from the actual value of an indicator for a dekade; "X(Y,P) - Average(P)".

#### 4.4.1. TAMSAT rainfall Estimate and Rainfall Climatology

Based on TAMSAT rainfall estimate from 2000 to 2012, the first 13 dekads and the last 10 dekads of every year are considered to belong to the dry season. Even though rainfall in some parts of Amhara region is bimodal, the first rainy season (March-May) contribution to agricultural production is not significant. In North Gonder, TAMSAT could not capture the first rainy season continuously every year. Most part of North Gonder is highland and characterised by a wide range of topography which reaches to 4600 at Mount Rasdashen. TAMSAT considers cloud top temperature whereas the rains during this season could be as a result of orographic effects. When east and south-easterly winds blow from the Indian Ocean and reach the central highlands of Ethiopia, these winds are forced to rise because of the high mountains. For some years (2004, 2005, 2007 and 2008), TAMSAT captured some rainfall during the first rainy seasons. In the identification of below and above average dekades for North Gondar using the TAMSAT rainfall estimate the average of all dekades from 2000 to 2012 and TAMSAT climatology 1983-2012 are used.

When the average of the rainfall estimate (figure 15) is considered from the 20th to 25th dekade of the years when maximum rainfall is expected, actual rainfall is lower than average rainfall. For the years 2002, 2004, 2005, 2007 and 2009 actual rainfall is below the average during dekades of high rainfall. All the remaining years also have some periods which show below average rainfall, either at the beginning of the rainy season or at the end of rainy season, or both. Even though the number of dekades (five) is representing a short period of time, it coincides with the starting time of the growing season in the area (June-October), and its effect on agricultural production is higher than below average dekades occurring during the dry season (November to May). Dekades during 2009 when high rainfall is expected are severely below average. The rain started early and continued for extended period of time. The calculated anomalies using TAMSAT RFE show below and above average values.

TAMSAT rainfall climatology of 30 years (figure 16) is also used to identify dekades which have below average rainfall and how long this below average continues. Based on the TAMSAT RFE climatology, during the mid of the growing season (from 19th to 24th dekades) of each year, the rainfall is far below climatology and this is because of high rainfall during these dekades in the 1980s and 1990s. High rainfall amounts during years prior to the year 2000 are not supported by in-situ data. Dekades at the beginning of the main rainy season (14th -17th) and dekades at the end of the rainy season (26th -28th) of many years are near normal compared to the climatology. The numbers of below average dekades identified using 30 years of TAMSAT rainfall climatology is higher compared to the number of below average dekades when the average of 13 years TAMSAT rainfall estimate is used.

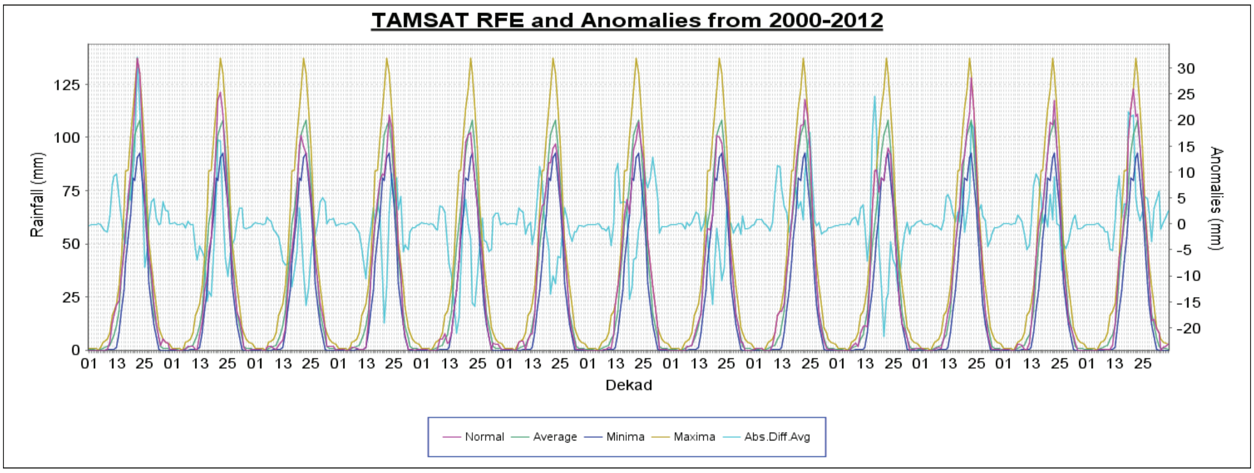


Figure 15 TAMSAT RFE and anomalies for North Gonder

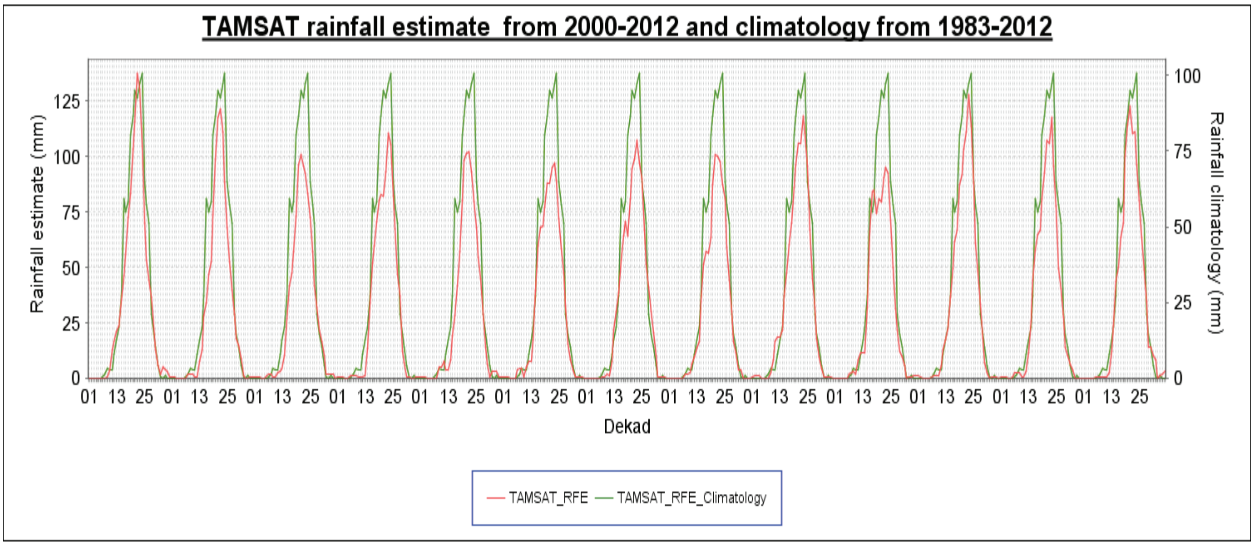


Figure 16 TAMSAT RFE and climatology for North Gonder

#### 4.4.2. FEWSNET Rainfall Estimate

Eleven years of processed dekadal FEWSNET rainfall estimates (figure 17) shows that many dekades of 2004, 2009 and 2011 are below average. Especially dekades in 2009 are facing a high variability of rainfall. According to the average values, some dekades of some years have rainfall amount below the average during the start of the rainy season, mid of the rainy season and/or during dekades at the end of the rainy season. Climatology of the FEWSNET rainfall estimate (Figure 18) is also used to identify below and above normal climatology dekades of years under consideration. Most of the dekades of the years 2004, 2005, 2011 have anomalies far below the climatology. The years 2006, 2007, 2008 and 2012 show that many dekades have relatively high negative anomalies especially from dekads 18 to 27 of all years which have high rainfall amount. The overall tendency is therefore similar with the result obtained using TAMSAT rainfall climatology (section 4.4.1.).

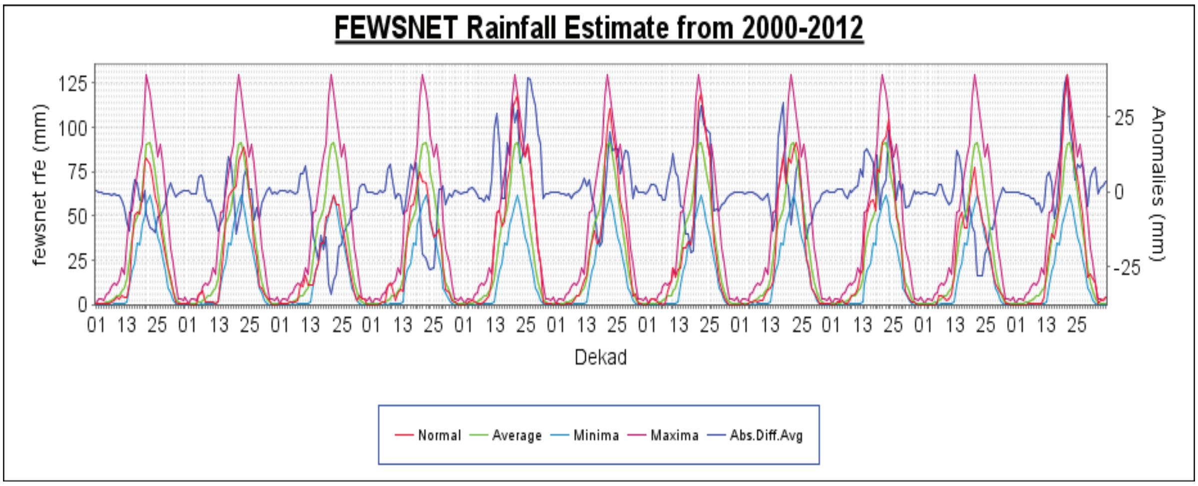


Figure 17 FEWSNET RFE and anomalies for North Gonder

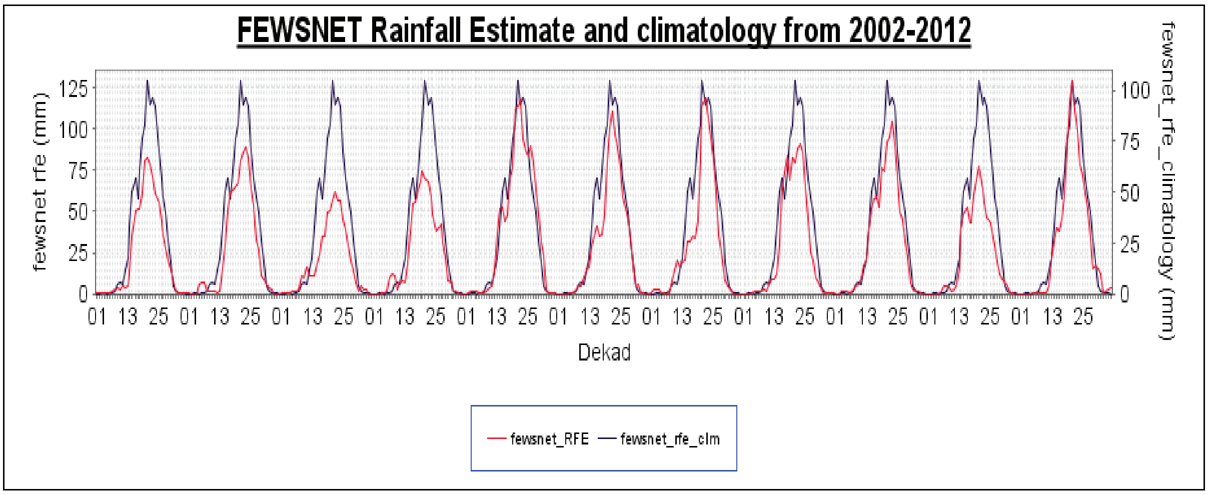


Figure 18 FEWSNET RFE and climatology for North Gonder

### 4.4.3. MOD16 Evapotranspiration

Average ET of 13 years data is used (figure 19). The maximum average evapotranspiration is 30.6 mm per dekade whereas the minimum value is 1.7 mm per dekade. Evapotranspiration is mainly governed by availability of water and evaporation demand of the atmosphere. Because of these reasons, evapotranspiration is high during the rainy seasons. Eventhough the evaporative demand of the atmosphere is high during the summer seasons (November to May), the water available to be evaporated and transpired is small (below 5 mm per dekade). However it reaches 38 mm per dekade during the rainy seasons. The negative and positive anomalies calculated indicate dekades which are below and above average ET values respectively. Similar to the indicators described above (section.4.4.1 and 4.4.2), many dekades of every year show below average values. More frequently, very low actual evapotranspiration values are estimated during the start and end of the rainy seasons (for example during 2001, 2002, 2004, and 2009).

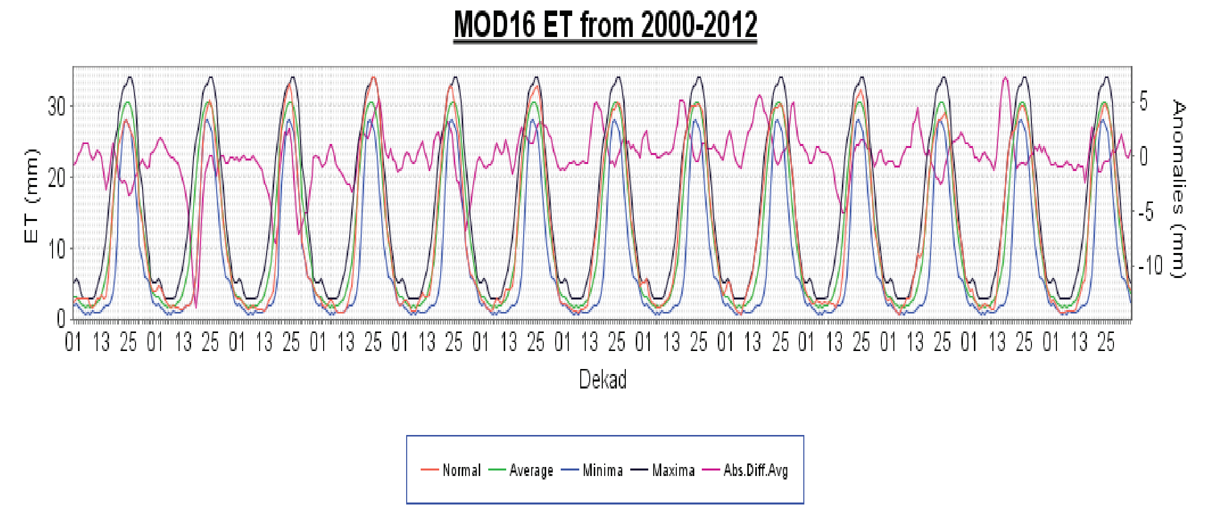


Figure 19 MOD16 Evapotranspiration for North Gonder

#### 4.4.4. MOD16 Potential Evapotranspiration

Unlike evapotranspiration, potential evapotranspiration is high during seasons when the availability of water is scarce and this is due to the evaporative demand of the atmosphere. Similar to sections (4.4.1, 4.4.2 and 4.4.3), average values of all dekades during thirteen years are used (figure 20). Summer season is dryer compared to the winter season in North Gonder so the amount of PET is higher in summer than the water evaporated and transpired during the winter season. Based on the anomalies calculated, those dekades which have negative values are below average whereas dekades which have positive anomalies are above average. Accordingly, all years have above average dekades. However, above average values estimated for some dekades of 2004, 2005 and 2009 are more near normal than for other years. Some dekades of 2001, 2002 and 2007 are affected by far above average values for more than a dekade. Therefore positive and negative anomalies indicate above average and below average actual PET values. Almost in all years, the PET is high from January to May.

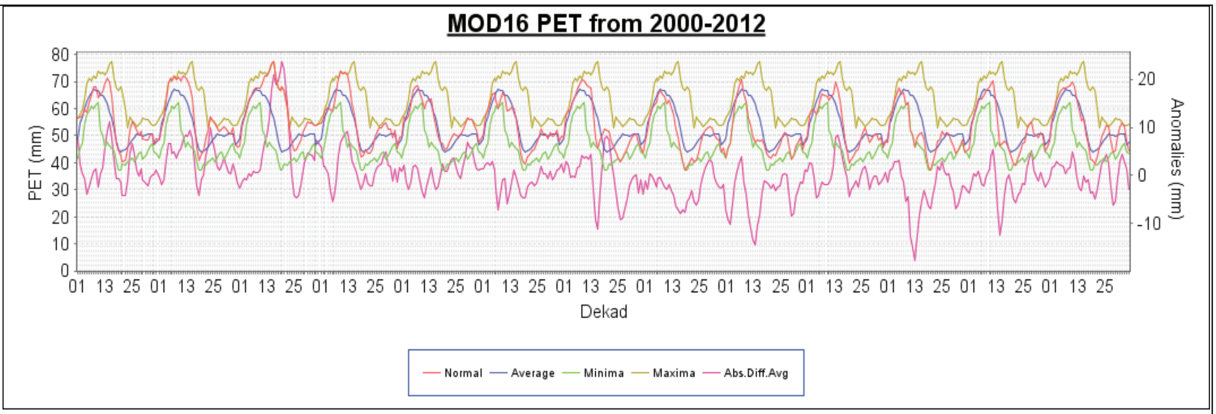


Figure 20 MOD16 potential evapotranspiration and anomalies for North Gonder

#### 4.4.5. FEWSNET Potential Evapotranspiration

According to the average values, many dekades of 2004, 2005 and 2006 have relatively lower actual PET whereas almost all dekades of 2011 and 2012 are above average. Some dekades of 2002, 2003, 2008 and 2011 have high peak of actual PET and the lowest actual PET occurred in 2004. Similar to section 4.4.4, low potential evapotranspiration means either the evaporative demand of the atmosphere is low or fulfilled by the available water on the area. Positive PET anomalies and negative anomalies of dekades indicate that the actual PET of the dekades was above and below the average respectively. Far below average anomalies occurred during the dekades of 2002, 2003, 2005 and 2007. Almost in all years PET is high during dekades from January to May.

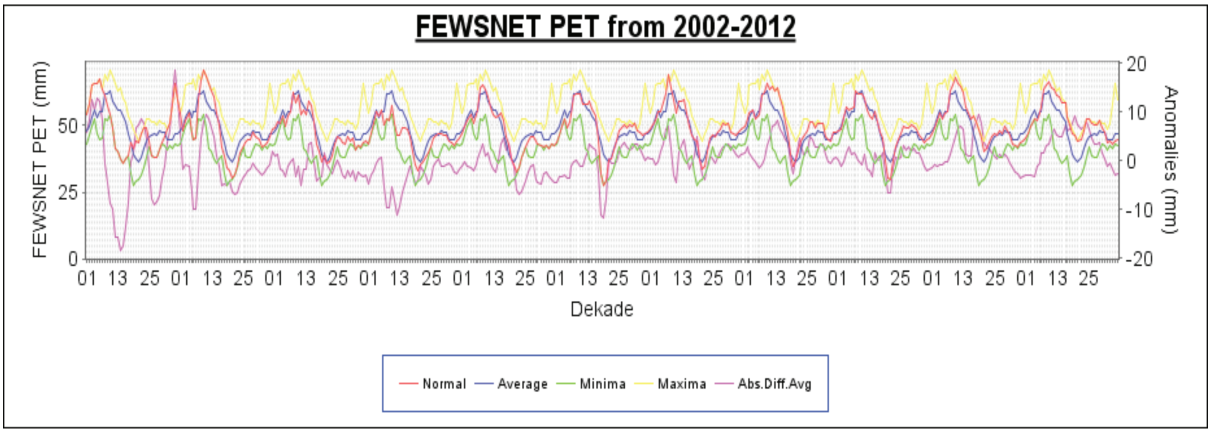


Figure 21 FEWSNET potential evapotranspiration for North Gonder

#### 4.4.6. eMODIS NDVI

According to the average dekadal values (figure 22), of 11 years, crop initial stages ($16^{th}$ -$18^{th}$ dekades) of the first four years (2002, 2003, 2004 and 2005) have below average NDVI. The anomalies calculated during these dekades also show low negatives. However, the remaining dekads of those years show above average NDVI. In 2007, the first few dekades are above average NDVI. Starting from 24th dekade of 2008 until the end of the growing season, and until $22^{nd}$ dekade of the next year, negative anomalies prevailed for an extended period of time. All the anomalies of these dekades are below zero. All dekades of 2010 are near normal below average. The deviation of actual NDVI of $17^{th}$ -$28^{th}$ dekades in 2011 is different from all other years. Based on the anomalies calculated, 2011 and 2012 have dekades whose anomalies are far above normal. The highest below average deviation occurred in 2009. The deviation from the average during the growing seasons of 2007 and 2010 show near normal conditions.

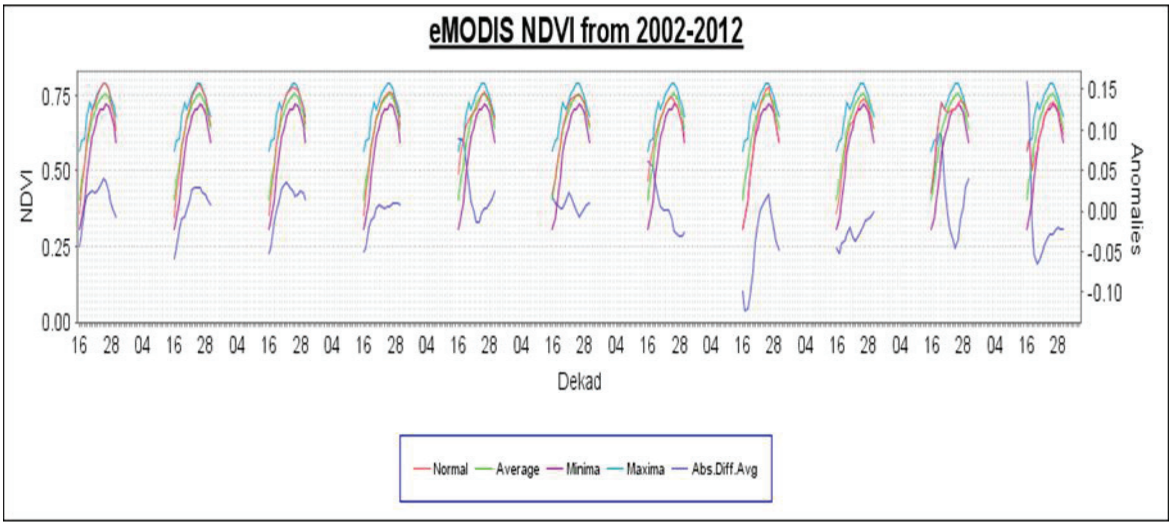


Figure 22 eMODIS NDVI for growing seasons (June-October) for North Gonder

## 4.5. Selection of indicators

According to the indicators discussed in section 4.4, dekades which have actual values below or above the average are identified using the anomalies calculated. However, according to the definition of drought given in section 1, the actual value of a single indicator for a period of time which is either normal, below or above the average does not indicate if there was drought or not. The length of the period of time should be also considered. Beyond that, because of its relationship and dependency with different factors, the identification of drought and non-drought conditions using a single indicator can lead to wrong conclusions. A higher confidence can be assigned if a period of time (multiple dekades) is identified as drought using two or more indicators. If most of the indicators converge and identify a period of time as having relevant anomalies, this assures that there are drought conditions.

The indicators used in identifying drought have to be different both in type /processes/ and the methods applied in estimating these processes. In selecting best indicators for drought identification using multiple indicators, FEWSNET and TAMSAT RFE are validated for the rainy season of 2010. The correlation coefficients obtained are 0.91 and 0.93 for FEWSNET and TAMSAT RFE respectively. Rainfall overestimated by FEWSNET RFE is high compared to TAMSAT RFE. The comparison of PET satellite products against Enku's ETo in section 4. 3.4 showed that FEWSNET PET has smaller correlation coefficients $R^2$ =0.72 compared to MOD16 PET correlation coefficients $R^2$ =0.74. The spatial resolution satellite product is also considered as criteria. The spatial of resolution FEWSNET PET (one degree) is lower than MOD16 (1 km). FEWSNET RFE has low spatial resolution (0.1 degree) when compared to TAMSAT RFE (0.0375 degree). Both PET and rainfall products are highly correlated and therefore show redundant information.

### 4.6. Combined indicators to assess drought

NDVI values have been decreasing from 2002 to 2012 except during 2009 whereas TAMSAT has been fluctuating. Dekades of 2002, 2005, 2007 and 2009 have relatively low rainfall peaks and extended rainfall periods compared to the other years. Figure 23 (a) also shows eMODIS NDVI values start to increase after two to three rainfall dekades. In 2002, 2005, 2007 and 2009 years which have low peaks of rainfall, eMODIS shows high NDVI values (figure 23 (a)). Therefore NDVI value is not only dependent on peaks of rainfall amount but also its onset and for how long it continued. Dekades of the year 2009 shows that the rainfall started earlier and ended later than other years so that high NDVI values are observed. This is because of the sensitivity of the crops to drought at early stage. Other factors that can lead to such indirect relationship of rainfall and NDVI can be due to agricultural practices.

Eventhough evapotranspiration is high when plenty of water is available, it does not exactly coincide with dekades of high rainfall. Especially, at the beginning the rainy season, while rainfall is increasing significantly, the amount of water evaporated and transpired did not increase as much as the rainfall. Because of dry conditions prior to the rainy season, infiltration, surface and sub-surface runoffs take the lion-share during the beginning of rainy season. The plant is also at infant stage. As presented in the figure 23 (b) below, evapotranspiration is not reducing immediately when rainfall is decreasing the amount of water stored in the crop root zone (and soil) is used. Evapotranspiration is continuously increasing for some time, and at later stage, it starts to diminish when the water available is being exploited by plants and the atmosphere. Because of the short rainfall period and low rainfall amount in 2001, 2002 and 2004, evapotranspiration has low peaks and continued for a shorter period of time. In 2009, even though the peak of rainfall is low, because of extended rainfall period, ET had higher peak and continued for a relatively longer period of time compared to 2001.

The highest peak of MOD16 PET is observed in 2002 whereas the lowest is in 2010. In 2004 and 2005, the temporal variability of PET was high. Because of the variability of the atmospheric weather, MOD16 PET had higher temporal variability than MOD16 ET. When potential evapotranspiration decreases during rainy season, actual evapotranspiration increased (figure 23 (c)). The two processes are opposite in time.

The combination between MOD16 ET and eMODIS NDVI (figure 23 d) during the growing seasons show that ET increases when NDVI increases almost all the time. During these dekades which show the direct relationship between MOD16 ET and eMODIS NDVI, most of ET is mainly from the vegetation. In 2003, ET increased as NDVI increased and later, ET diminished immediately following the change in NDVI. But, in 2007, ET was at maximum peak for some dekades because of high NDVI continued for some dekades. Such direct relationship also occurred in 2009 when ET deviates following the deviation in NDVI.

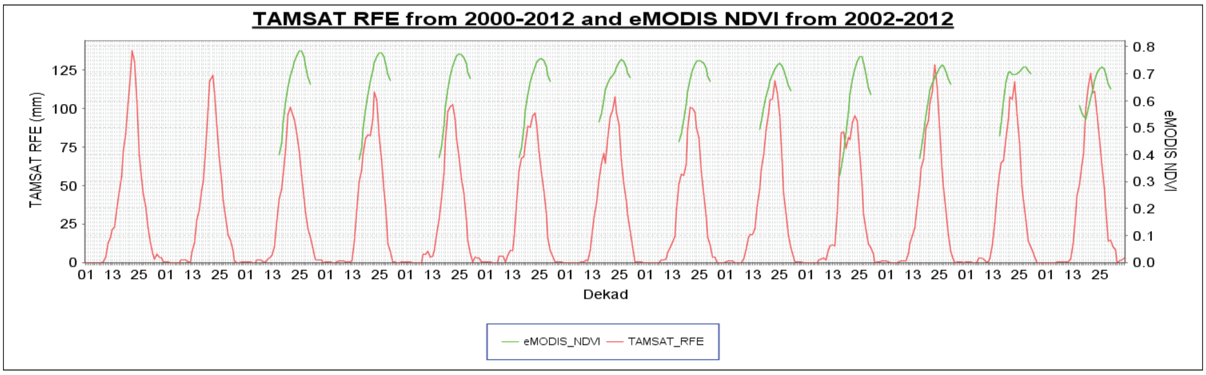


(a)

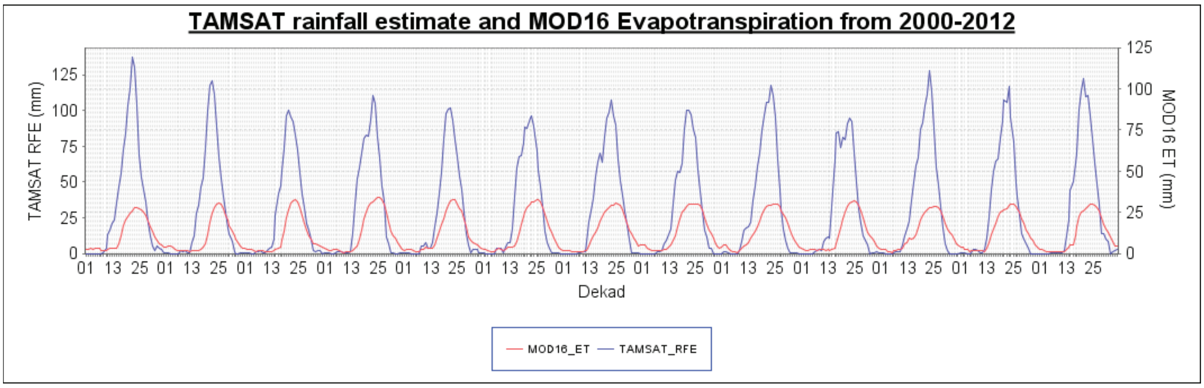


(b)

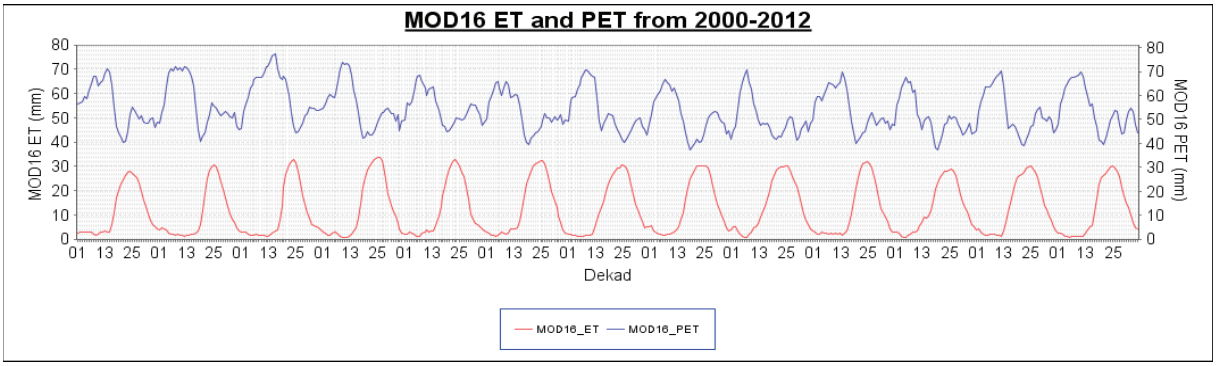


(c)

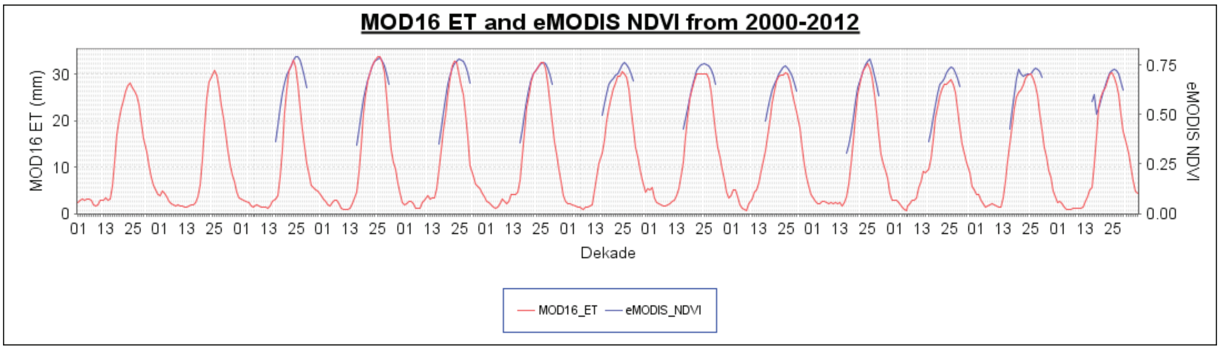


(d)

Figure 23 Combination of indicators (a) TAMSAT RFE and eMODIS NDVI, (b) TAMSAT RFE and MOD16 evapotranspiration, (c) MOD16 ET and PET, (d) MOD16 ET and eMODIS NDVI of North Gonder

The following figure shows the number of below average (for TAMSAT, eMODIS NDVI and MOD16 ET) and above average (for MOD16 PET) dekades during the growing seasons (June to October) of each year since 2000. Eventhough there are differences in the number of dekades counted as below and above average per growing season for ET and PET respectively, MOD16 ET and PET are almost similar in trend. The differences are mainly occurring in 2002 and 2010. There is also similarity in trend between the number of below average dekades counted per growing season using TAMSAT and eMODIS anomalies. The number of below average dekades counted during the growing seasons of 2007, 2008 and 2010 is leading to differences in their trend over time.

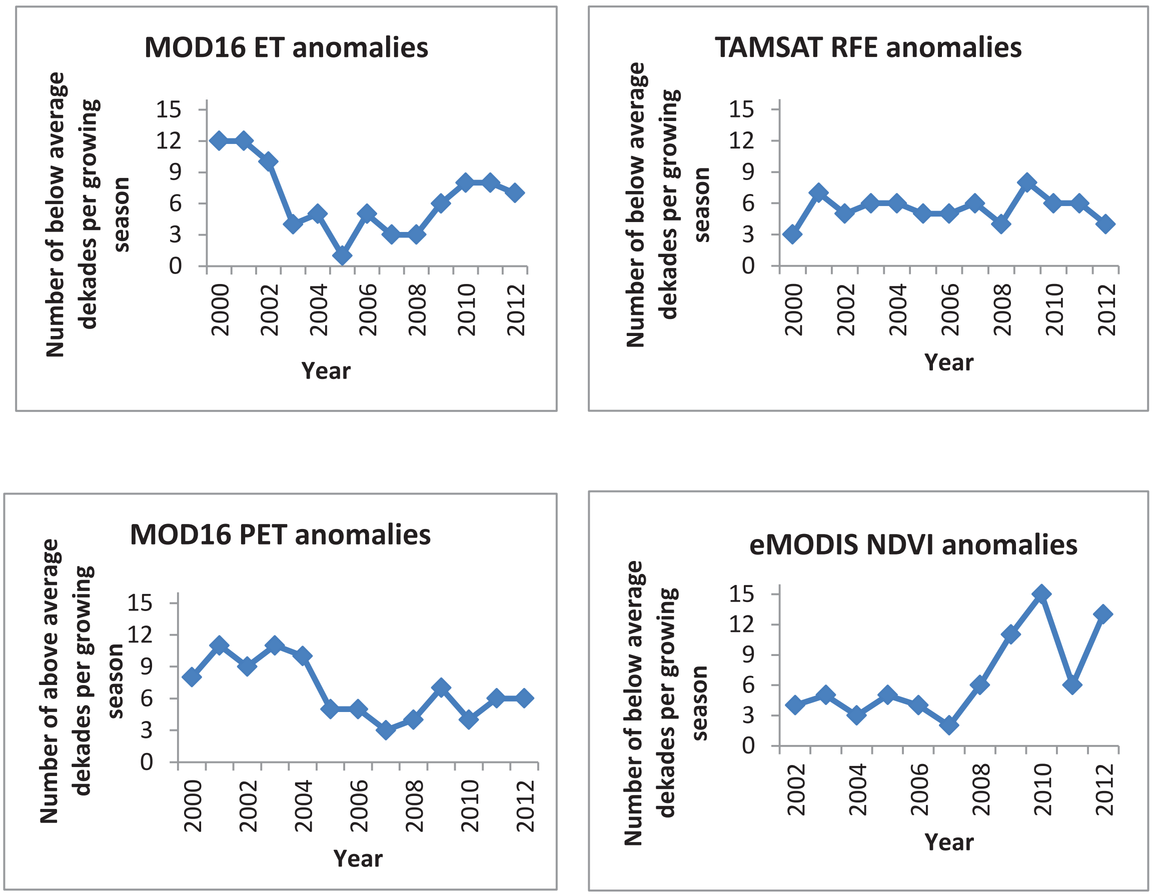


Figure 24 Number of dekades below average (TAMSAT RFE, MOD16 ET eMODIS NDVI) and above average (MOD16 PET) counted per growing season of each year of selected indicators for North Gonder

#### 4.6.1. Drought identification using multiple indicators

Figure 25 shows below and above average anomalies with respect to the normal conditions. In 2002 and 2009, MOD16 PET has above average anomalies which are far from the average whereas during some dekades of 2006, 2008 and 2010, shows below average anomalies which are far from the normal conditions. Above average anomalies which are very far from the average of TAMSAT RFE and very far negative anomalies from the average of MOD16 ET are seen in 2000, 2001, 2009 and 2012, and 2001, 2002 2004 and 2005 respectively. Because of small values of actual MOD16 ET, the deviations in both below and above average are not as large as TAMSAT and PET deviations.

The anomalies of eMODIS NDVI are calculated only for the growing season (June to October). The combinations between anomalies of TAMSAT rainfall and MOD16 ET, and MOD16 ET and PET are for 13 years (2000 to 2012) while others start from 2002. Based on combinations of anomalies of MOD16 ET and PET (figure 25 a), if dekades have anomaly values of ET and PET below and above normal respectively for a period of time, there was drought. TAMSAT and MOD16 ET (figure 25 b), the fourth combination of indicators MOD16 ET and eMODIS NDVI (figure 25 c) and TAMSAT and eMODIS NDVI (figure 24 d) show dekades which have anomalies below and above average, and how far these deviate from normal conditions. In 2010 and 2012, almost all dekades of the growing seasons have near normal below average NDVI values (figure 25 d). The rainfall decreased when the crops were at infant stage. The rainfall started to decrease as the end of the growing season is approaching while NDVI values start to recover. Due to high sensitivity of crops during germination period, low rainfall events which occur during crops early stage are more Sever.

Table 5 shows drought events identified using multiple indicators which occurred during the growing seasons of 13 years. Anomalies of TAMSAT RFE, MOD16 ET, MOD16 PET and eMODIS NDVI are used in identifying these drought events. If two or more consecutive dekades are below average (above average for MOD16 PET) and these are identified by two or more indicators, there is a high probability of drought. The growing seasons of 2001, 2002, 2003 and 2009 are affected by drought during the first few dekades whereas for the remaining years, drought occurred during mid and later stages of the growing seasons. The growing seasons of 2005 and 2007 were relatively unaffected by drought. The colours assigned for the cells in the table show for how many dekades anomalies of each indicators continues.

For North Shewa which is located to southwest of Amhara region, in drought temporal trend analysis, all the indicators (appendix C) are highly variable overtime. This is because of its location to the edge of the Rift valley. The eastern part of North Shewa receives relatively warm winds from Indian Ocean. When these winds blow over the central highlands, they start to cold and precipitate to the central and western part of Amhara region. Following this temporal change in rainfall over North Shewa, all other indicators are varying overtime. As confirmed by the in-situ data, the rainfall climatology in North Shewa is bimodal. This bimodal nature of rainfall is well estimated by TAMSAT and FEWSNET RFE. But, because of its closer location to eastern Rift valley, the peaks of high rainfall are low compared to North Gonder. High rainfall events (>50 mm) occurred only for few dekades in North Shewa whereas in North Gonder, a number of dekades at which high rainfall events recorded are many per growing season. Because of plateau nature of the area, the occurrence of orographic rainfall is low. The bimodal nature of rainfall is also reflected by MOD16 ET and NDVI value of North Shewa. The NDVI value increases following the first rainy season and it starts to diminish during the transition period from the first rainy season to the second rainy season. Following the significant amount of water contributed to ET prior the main growing season, ET also has two peaks per a year. Both MOD16 and FEWSNET PET satellite products behave opposite to ET in time.

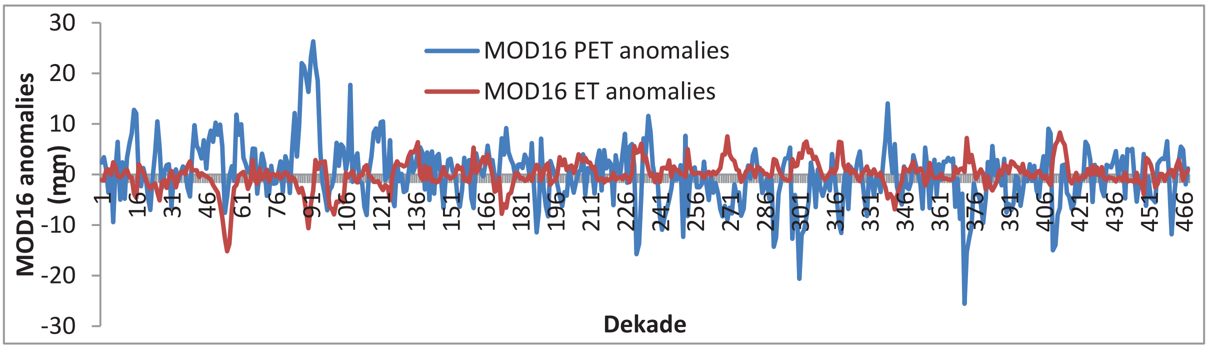


(a)

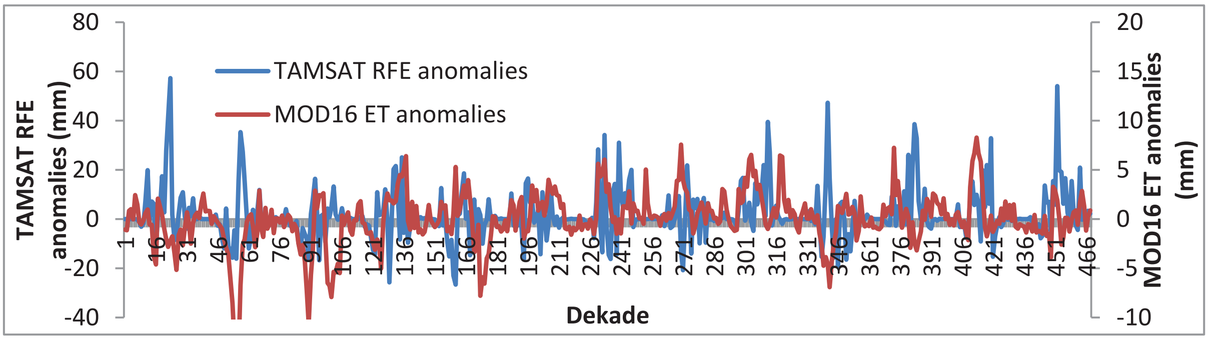


(b)

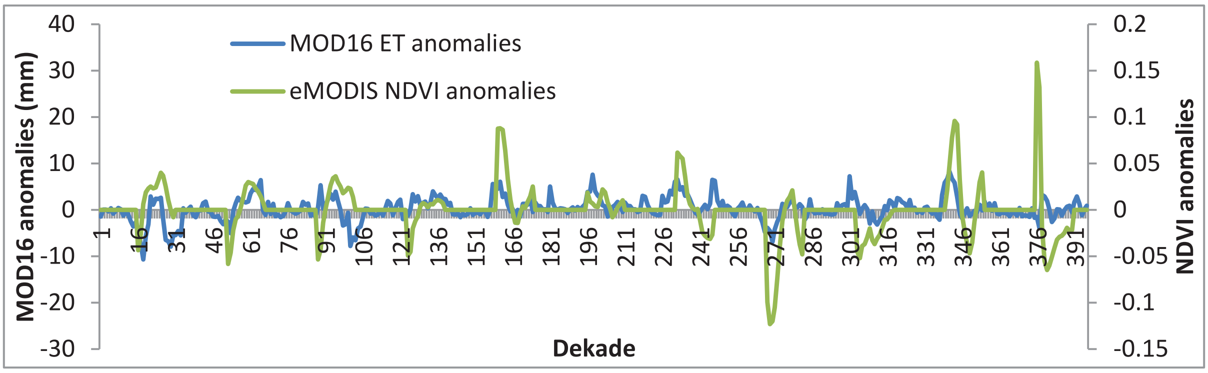


(c )

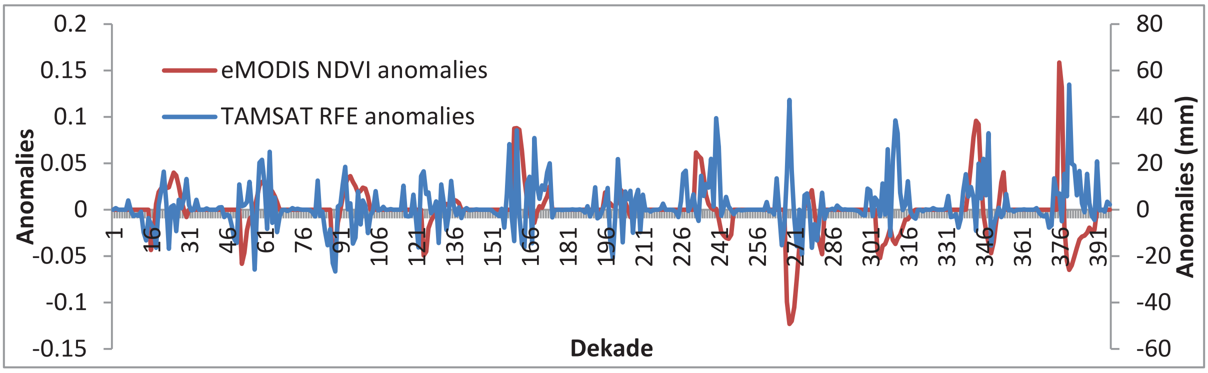


(d)

Figure 25 Drought identification using multiple indicators (a) MOD16 ET and PET anomalies, (b), TAMSAT and MOD16 ET anomalies (c ) MOD16 ET and eMODIS NDVI anomalies, (d) TAMSAT and eMODIS NDVI anomalies of North Gonder

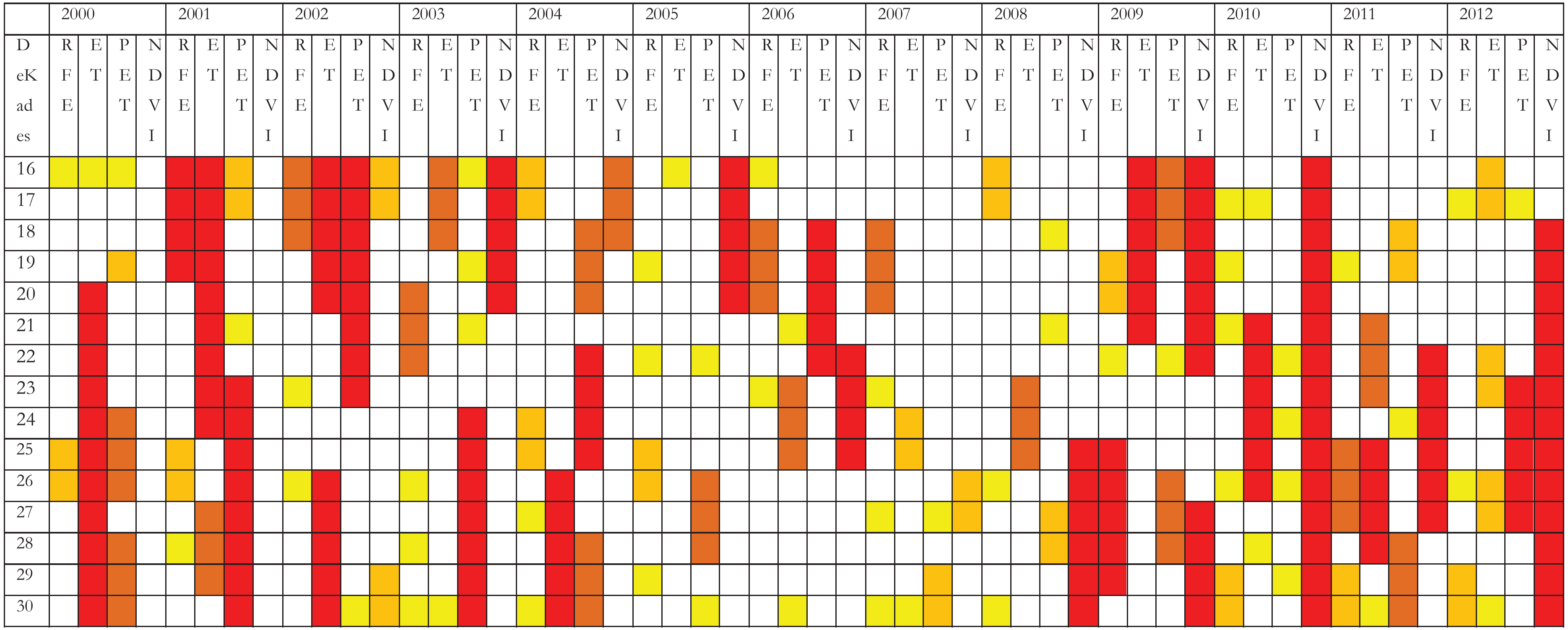


RFE=TAMSAT below average anomalies, ET=MOD16 ET below average anomalies, PET=MOD16 PET above average, NDVI= eMODIS NDVI below average anomalies

Legend

1 dekade 2 dekades 3 dekades >=4 dekades

Table 5 The below average (TAMSAT RFE, MOD16 ET eMODIS NDVI) and above average (MOD16 PET) dekades and their duration per growing season for selected indicators for North Gonder from 2000 to 2012

# 5. CONCLUSION AND RECOMMENDATION

## 5.1. Conclusion

All the selected gauge stations used in this study are good in representing the reality. This is confirmed by double-mass curve analysis. All the gauge stations have high correlation with the mean monthly rainfall of the region. Even though the spatial distribution of gauges is scarce and random, they are able to indicate most drought prone areas (east and north eastern parts) of the region. Based on monthly rainfall climatology of the region, the second rainy season (June to October) has higher rainfall for an extended period of time compared to the first rainy season (March to May). The pixel to point validation of TAMSAT rainfall climatology conducted for the whole region using the average values of stations for the rainy season showed a high correlation coefficient. The correlation coefficient calculated for TAMSAT rainfall estimates and gauges monthly rainfall for 2010 also showed direct and strong relationship. Comparison between TAMSAT climatology and ARC2 climatology also shows a direct relationship and a very good correlation coefficient. Both climatology products have good correlation in presenting low rainfall amounts.

Reference evapotranspiration calculated using the Enku method showed good performance in estimating potential evapotranspiration during rainy and dry seasons. Accordingly, calculated reference evapotranspiration is low during wet seasons for all stations except Combolcha station. Comparison of Enku's calculated reference evapotranspiration and FEWSNET PET showed a lower correlation coefficient than the comparison between Enku's ETo and MOD16 PET. Eventhough the comparison done between MOD16 PET and FEWSNET PET using their actual spatial resolution already showed a very good correlation coefficient, this correlation coefficient is further improved after MOD16 PET is aggregated to one degree spatial resolution.

TAMSAT RFE, FEWSNET RFE, FEWSNET PET, eMODIS NDVI, MOD16 ET and PET are used to identify below average and above average dekades separately. According to TAMSAT and FEWSNET rainfall climatology, most dekades of all the years have anomalies below average. It indicates that years prior to 2000, had relatively above average TAMSAT and FEWSNET rainfall estimates. eMODIS NDVI showed that most dekads which had below average values are mostly the first few dekads of a growing season. NDVI value showed that it also depends on the onset of rainfall in addition to the amount of rainfall. MOD16 ET and PET products showed that they behave opposite in time. When ET increased PET decreased.

Because of their low spatial resolution, FEWSNET RFE and FEWSNET PET are neglected in drought event identification analysis using multiple indicators. Drought identification using TAMSAT RFE, eMODIS NDVI, MOD16 ET and PET is done only for the growing seasons (June to October) of each year. The anomalies and to what extent they deviate from the average are presented in figure 24. Combined anomalies of MOD16 ET and PET, TAMSAT RFE and eMODIS NDVI, and TAMSAT RFE and MOD16 ET, (figure 23) show good similarity in trend especially during the growing seasons. The combination of anomalies of MOD16 ET and eMODIS NDVI follow very similar trend when compared to other combination of anomalies. There is similarity in trend across the selected indicators over time even though there are differences in the number of dekades which had below average (for TAMSAT RFE, eMODIS NDVI and MOD16 ET) and above average values (for MOD16 PET) per growing season.

In table 5, dekades which had below average (for TAMSAT RFE, eMODIS NDVI and MOD16 ET) and above average (for MOD16 PET) values, and their duration is presented. Therefore, if two or more indicators identify a number of consecutive dekades which have below average values (for TAMSAT RFE, eMODIS NDVI and MOD16 ET) and above average values (for MOD16 PET), it enforces the likelihood of occurrence of drought during that time. Accordingly, the growing seasons of 2005 and 2007 were relatively unaffected by drought, 2006 and 2008 are slightly affected. Most dekades of other growing seasons were repeatedly affected by drought. 2001, 2002, 2003 and 2009 are among years when drought occurred during the first few dekades whereas during 2000, 2004 and 2011, the last few dekades were drought affected.

In conclusion, all the validations and the comparisons done showed a good correlation coefficient and direct relationship. Most of the time some of the indicators used in drought assessment showed the expected inter-relationship. Drought has occurred repeatedly during the first few dekades of some growing seasons and as well as during the middle or towards the end.

### 5.2. Recommendation

The availability of meteorological data is limited both in space (sparse distribution of meteorological stations) and time (there are no complete and long-time recorded data).

- High temporal scale (at least dekadal) in-situ data would enable a more detailed assessment compared to the temporal scale (monthly) which is used by the data sharing policy of Ethiopian NMA.
- Increasing the number of meteorological stations in the region is important and it increases the spatial reliability of these types of studies and it will lead to better result so that the decisions and interventions can be done with higher confidence. Improving both the number and distribution of gauges will enable to better validate and calibrate satellite products.

- The PET estimates made using MOD16 are higher compared to FEWSNET. As far as both MOD16 and FEWSNET are estimating the same hydrological process, it would be more convenient if the difference between these estimates is further investigated.
- Eventhough resampling is applied, some of the satellite products (FEWSNET PET) used have low spatial resolution. The effect of low spatial resolution of satellite products is greater for the Amhara region where the topographical conditions show large variations and consequently influences the actual earth surface processes. Improved spatial resolution of satellite products would likely lead to better accuracy in retrieving required spatio-temporal information.
- It is also important to investigate the reduction in agricultural yield as a result of drought events occurred in growing seasons.

# LIST OF REFERENCES


Abraha, M. E. (2013). *Assessment of drought early warning in Ethiopia : a comparison of WRSI by surface energy balance and soil water balance.* University of Twente Faculty of Geo-Information and Earth Observation (ITC), Enschede. Retrieved from http://www.itc.nl/library/papers_2013/msc/wrem/abraha.pdf

Alireza, S., & Josef, E. (2013). Spatio-Temporal Analysis of Droughts in Semi-Arid Regions by Using Meteorological Drought Indices. *Atmosphere, 4*(2), 94-112.

Araya, A., & Stroosnijder, L. (2011). Assessing drought risk and irrigation need in northern Ethiopia. *Agricultural and Forest Meteorology, 151*(4), 425-436. doi: http://dx.doi.org/10.1016/j.agrformet.2010.11.014

Badripour, H. (2007). Role of Drought Monitoring and Management in NAP Implementation. In M. K. Sivakumar & N. Ndiang'ui (Eds.), *Climate and Land Degradation* (pp. 565-582): Springer Berlin Heidelberg.

Belayneh, A., Adamowski, J., Khalil, B., & Ozga-Zielinski, B. (2014). Long-term SPI drought forecasting in the Awash River Basin in Ethiopia using wavelet neural network and wavelet support vector regression models. *Journal of Hydrology, 508*(0), 418-429. doi: http://dx.doi.org/10.1016/j.jhydrol.2013.10.052

Berhan, G., Hill, S., Tadesse, T., & Atnafu, S. (2011). Using Satellite Images for Drought Monitoring: A Knowledge Discovery Approach. *Journal of Strategic Innovation & Sustainability, 7*(1).

Bewket, W., & Conway, D. (2007). A note on the temporal and spatial variability of rainfall in the drought-prone Amhara region of Ethiopia. *International Journal of Climatology, 27*(11), 1467-1477.

Biswas, S., Roy, S., & Sarkar, S. (2013). Drought Risk Assessment Using GIS and Remote Sensing. In S. Chakraborty & G. Bhattacharya (Eds.), *Proceedings of the International Symposium on Engineering under Uncertainty: Safety Assessment and Management (ISEUSAM - 2012)* (pp. 849-857): Springer India.

Brown, J., Jenkerson, C., & Gu, Y. (2008). *Using eMODIS Vegetation Indices for Operational Drought Monitoring.* Paper presented at the NIDIS Workshop on Remote Sensing.

Byun, H.-R., & Wilhite, D. A. (1999). Objective quantification of drought severity and duration. *Journal of climate, 12*(9).

Chen, S.-T., Kuo, C.-C., & Yu, P.-S. (2009). Historical trends and variability of meteorological droughts in Taiwan/Tendances historiques et variabilité des sécheresses météorologiques à Taiwan. *Hydrological sciences journal, 54*(3), 430-441.

Climate Prediction Center. (2006, February 23, 2006). Africa RFE General Description. Retrieved January 5, 2013, from http://www.cpc.ncep.noaa.gov/products/fews/RFE2.0_desc.shtml

Dinku, T., Ceccato, P., Grover-Kopec, E., Lemma, M., Connor, S., & Ropelewski, C. (2007). Validation of satellite rainfall products over East Africa's complex topography. *International Journal of Remote Sensing, 28*(7), 1503-1526.

Dogan, S., Berktay, A., & Singh, V. P. (2012). Comparison of multi-monthly rainfall-based drought severity indices, with application to semi-arid Konya closed basin, Turkey. *Journal of Hydrology, 470–471*(0), 255-268. doi: http://dx.doi.org/10.1016/j.jhydrol.2012.09.003

Enku, T., & Melesse, A. M. (2013). A simple temperature method for the estimation of evapotranspiration. *Hydrological Processes.*

FAO. (2012). FAO Irrigation and Drainage Paper. from http://www.kimberly.uidaho.edu/ref-et/fao56.pdf

Gadisso, B. E. (2007). *Drought assessment for the Nile basin using meteosat second generation data with special emphasis on the upper Blue Nile region.* ITC, Enschede. Retrieved from http://www.itc.nl/library/papers_2007/msc/wrem/gadisso.pdf

Gebrehiwot, T., van der Veen, A., & Maathuis, B. (2011). Spatial and temporal assessment of drought in the Northern highlands of Ethiopia. *International Journal of Applied Earth Observation and Geoinformation, 13*(3), 309-321. doi: http://dx.doi.org/10.1016/j.jag.2010.12.002

Gelassie, T. Y. (2012). *Remote sensing evapotranspiration using geonetcast and in situ data streams for drought monitoring and early warning : case study for the Amhara region in Ethiopia.* University of Twente Faculty of Geo-Information and Earth Observation (ITC), Enschede. Retrieved from http://www.itc.nl/library/papers_2012/msc/wrem/tinebeb.pdf

Gray, C., & Mueller, V. (2012). Drought and Population Mobility in Rural Ethiopia. *World Development, 40*(1), 134-145. doi: http://dx.doi.org/10.1016/j.worlddev.2011.05.023

Grimes, D. I. F., Pardo-Igúzquiza, E., & Bonifacio, R. (1999). Optimal areal rainfall estimation using raingauges and satellite data. *Journal of Hydrology, 222*(1–4), 93-108. doi: http://dx.doi.org/10.1016/S0022-1694(99)00092-X

Hayes, M. J., Svoboda, M. D., Wilhite, D. A., & Vanyarkho, O. V. (1999). Monitoring the 1996 drought using the standardized precipitation index. *Bulletin of the American Meteorological Society, 80*(3), 429-438.

Herman, E., & Dominique, H. (2013). Software for the Processing and Interpretation of Remotely sensed Image Time Series user manual

Maathuis, B. H. P., Mannaerts, C., Schouwenburg, M., Retsios, B., Lemmens, R., & Nkeou, M. R. (2013). In Situ and Online Data Toolbox Installation, Configuration and User Guide. 1.3. from http://52north.org/communities/earth-observation/isod-toolbox

Maathuis, B. H. P., & Schouwenburg, M. (2013). Conversion Tool for Time Series Data Processing User Manua. Enschede: University of Twente, Faculty of Geo-Information Science and Earth Observation

Maggioni, V., Reichle, R. H., & Anagnostou, E. N. (2013). The efficiency of assimilating satellite soil moisture retrievals in a land data assimilation system using different rainfall error models. *Journal of Hydrometeorology, 14*(1), 368-374.

Maidment, R. I., Grimes, D. I. F., Allan, R. P., Greatrex, H., Rojas, O., & Leo, O. (2012). Evaluation of satellite-based and model re-analysis rainfall estimates for Uganda. *Meteorological Applications*, n/a-n/a. doi: 10.1002/met.1283

McKee, T. B., Doesken, N. J., & Kleist, J. (1993). *The relationship of drought frequency and duration to time scales.* Paper presented at the Proceedings of the 8th Conference on Applied Climatology.

Mirabbasi, R., Anagnostou, E. N., Fakheri-Fard, A., Dinpashoh, Y., & Eslamian, S. (2013). Analysis of meteorological drought in northwest Iran using the Joint Deficit Index. *Journal of Hydrology, 492*(0), 35-48. doi: http://dx.doi.org/10.1016/j.jhydrol.2013.04.019

Mkhabela, M., Bullock, P., Gervais, M., Finlay, G., & Sapirstein, H. (2010). Assessing indicators of agricultural drought impacts on spring wheat yield and quality on the Canadian prairies. *Agricultural and Forest Meteorology, 150*(3), 399-410. doi: http://dx.doi.org/10.1016/j.agrformet.2010.01.001

Mu, Q., Heinsch, F. A., Zhao, M., & Running, S. W. (2007). Development of a global evapotranspiration algorithm based on MODIS and global meteorology data. *Remote Sensing of Environment, 111*(4), 519-536.

Mu, Q., Zhao, M., & Running, S. W. (2011). Improvements to a MODIS global terrestrial evapotranspiration algorithm. *Remote Sensing of Environment, 115*(8), 1781-1800.

Nagarajan, R. (2010). Drought Indices *Drought Assessment* (pp. 160-204): Springer Netherlands.

Novella, N. S., & Thiaw, W. M. (2013). African Rainfall Climatology Version 2 for Famine Early Warning Systems. *Journal of Applied Meteorology & Climatology, 52*(3).

Owrangi, M. A., Jan, A., Mehrdad, R., Ali, M., & Sharifan, R. A. (2011). Drought Monitoring Methodology Based on AVHRR Images and SPOT Vegetation Maps. *Journal of Water Resource and Protection, 03*(05), 325-334.

Palmer, W. C. (1965). Meteorological drought. Research Paper No. 45. US Department of Commerce. *Weather Bureau, Washington, DC.*

Quiring, S. M., & Ganesh, S. (2010). Evaluating the utility of the Vegetation Condition Index (VCI) for monitoring meteorological drought in Texas. *Agricultural and Forest Meteorology, 150*(3), 330-339. doi: http://dx.doi.org/10.1016/j.agrformet.2009.11.015

Ramakrishna, G., & Demeke, A. (2002). An Empirical Analysis of Food Security in Ethiopia: The Case of North Wello. *Africa Development, 27*(1-2), 127-143.

Rhee, J., Im, J., & Carbone, G. J. (2010). Monitoring agricultural drought for arid and humid regions using multi-sensor remote sensing data. *Remote Sensing of Environment, 114*(12), 2875-2887. doi: http://dx.doi.org/10.1016/j.rse.2010.07.005

Rosell, S. (2011). Regional perspective on rainfall change and variability in the central highlands of Ethiopia, 1978–2007. *Applied Geography, 31*(1), 329-338. doi: http://dx.doi.org/10.1016/j.apgeog.2010.07.005

Spruce, J. P., Sader, S., Ryan, R. E., Smoot, J., Kuper, P., Ross, K., . . . Hargrove, W. (2011). Assessment of MODIS NDVI time series data products for detecting forest defoliation by gypsy moth outbreaks. *Remote Sensing of Environment, 115*(2), 427-437. doi: http://dx.doi.org/10.1016/j.rse.2010.09.013

Steinemann, A. C., Hayes, M. J., & Cavalcanti, L. (2005). Drought indicators and triggers. *Wilhite, D. Editor.*

Tonini, F., Jona Lasinio, G., & Hochmair, H. H. (2012). Mapping return levels of absolute NDVI variations for the assessment of drought risk in Ethiopia. *International Journal of Applied Earth Observation and Geoinformation, 18*(0), 564-572. doi: http://dx.doi.org/10.1016/j.jag.2012.03.018

Vasiliades, L., & Loukas, A. (2009). Hydrological response to meteorological drought using the Palmer drought indices in Thessaly, Greece. *Desalination, 237*(1–3), 3-21. doi: http://dx.doi.org/10.1016/j.desal.2007.12.019

Washington, R., Kay, G., Harrison, M., Conway, D., Black, E., Challinor, A., . . . Todd, M. (2006). African climate change: taking the shorter route. *Bulletin of the American Meteorological Society, 87*(10), 1355-1366.

White, D., & Walcott, J. (2009). The role of seasonal indices in monitoring and assessing agricultural and other droughts: a review. *Crop and Pasture Science, 60*(7), 599-616.

Wilhite, D. A. (2007). Drought. In J. Lidstone, L. Dechano & J. Stoltman (Eds.), *International Perspectives on Natural Disasters: Occurrence, Mitigation, and Consequences* (Vol. 21, pp. 147-162): Springer Netherlands.

Xie, P., & Arkin, P. A. (1996). Analyses of global monthly precipitation using gauge observations, satellite estimates, and numerical model predictions. *Journal of climate, 9*(4), 840-858.

Zhang, A., & Jia, G. (2013). Monitoring meteorological drought in semiarid regions using multi-sensor microwave remote sensing data. *Remote Sensing of Environment, 134*(0), 12-23. doi: http://dx.doi.org/10.1016/j.rse.2013.02.023

Zhao, Y., Li, S., & Zhang, Y. (2005). Early Detection and Monitoring of Drought and Flood in China Using Remote Sensing and GIS. In M. K. Sivakumar, R. Motha & H. Das (Eds.), *Natural Disasters and Extreme Events in Agriculture* (pp. 305-317): Springer Berlin Heidelberg.

APPENDEX A: Reliability of gauge stations

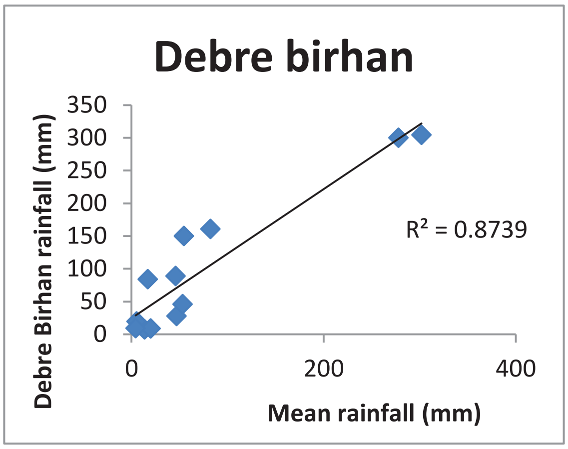


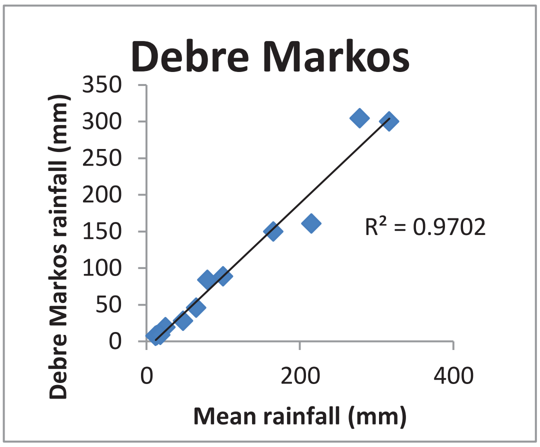


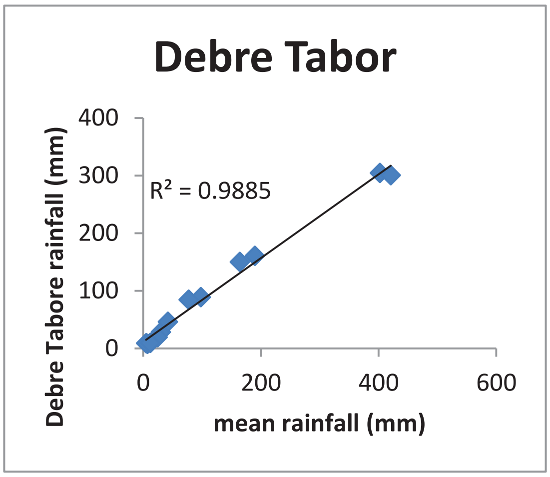


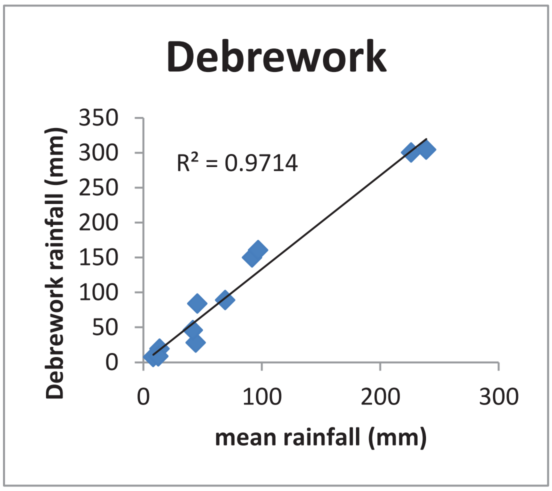


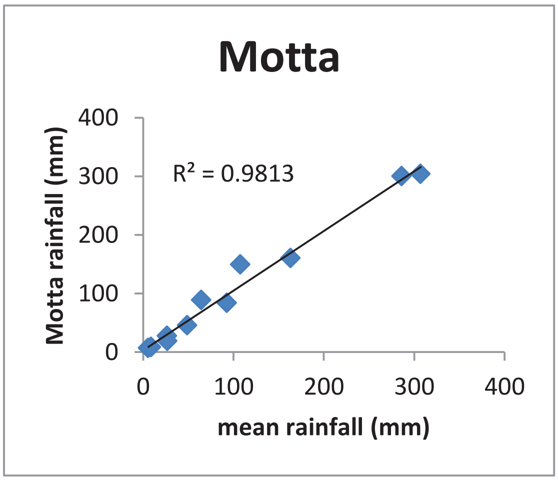


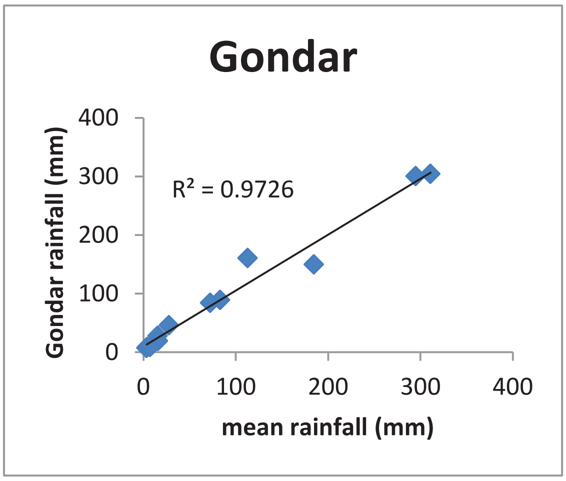

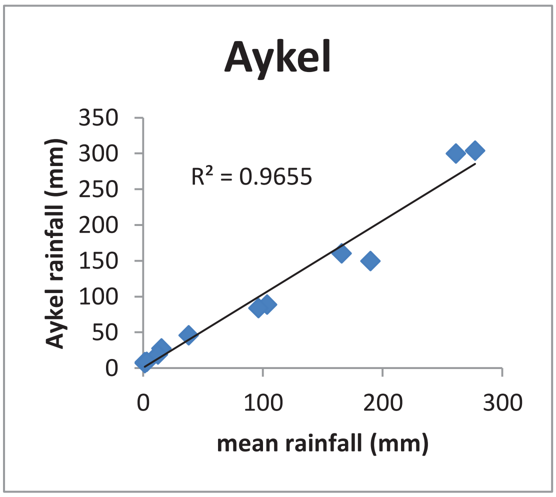
Aykel
R² = 0.9655
Aykel rainfall (mm)
mean rainfall (mm)
0
50
100
150
200
250
300
350
0
100
200
300

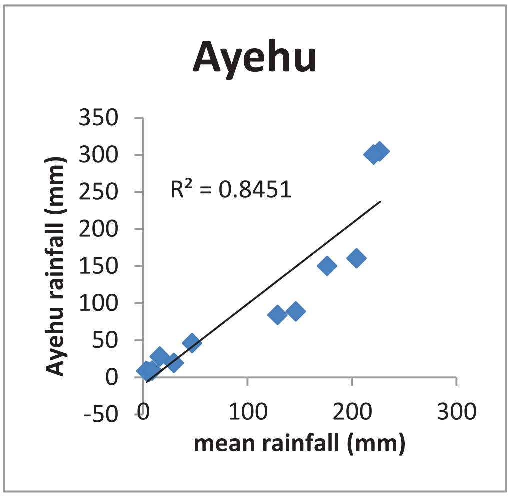
Ayehu
R² = 0.8451
Ayehu rainfall (mm)
mean rainfall (mm)
-50
0
50
100
150
200
250
300
350
0
100
200
300

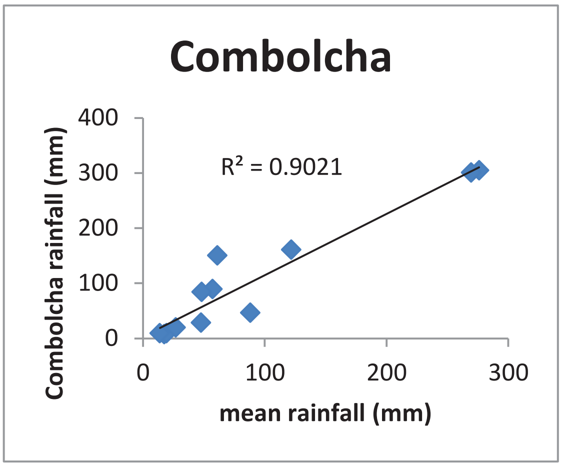
Combolcha
R² = 0.9021
Combolcha rainfall (mm)
mean rainfall (mm)
0
100
200
300
400
0
100
200
300

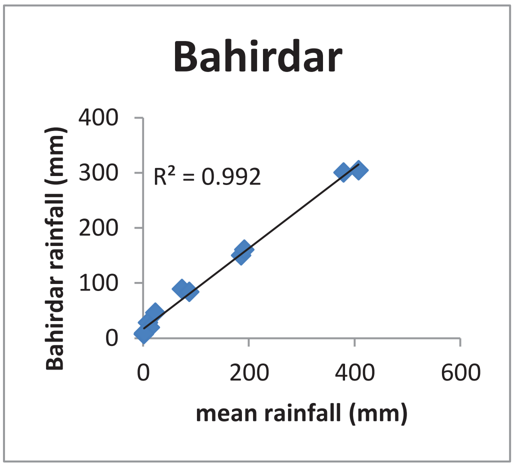
Bahirdar
R² = 0.992
Bahirdar rainfall (mm)
mean rainfall (mm)
0
100
200
300
400
0
200
400
600

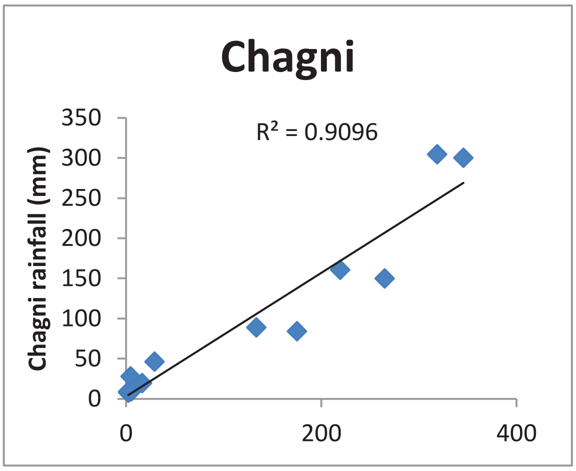
Chagni
R² = 0.9096
Chagni rainfall (mm)
0
50
100
150
200
250
300
350
0
200
400

APPENDEX B: Validation of TAMSAT rainfall

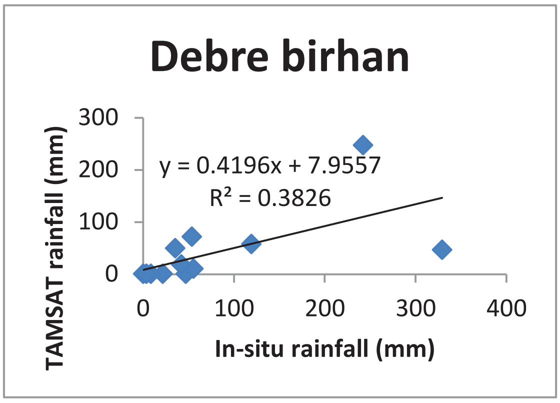


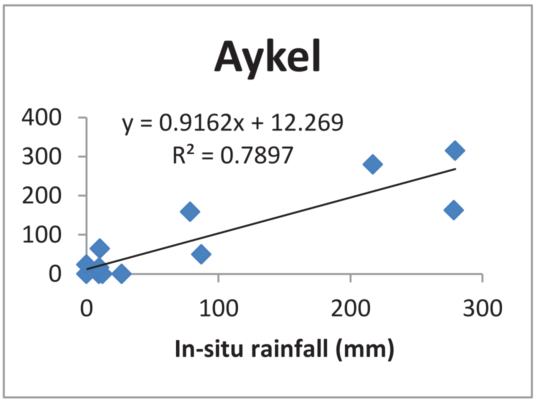


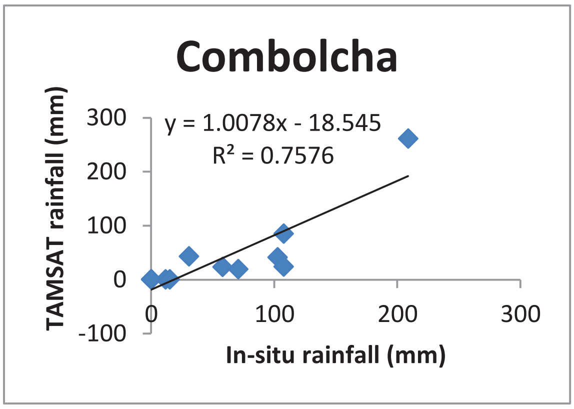


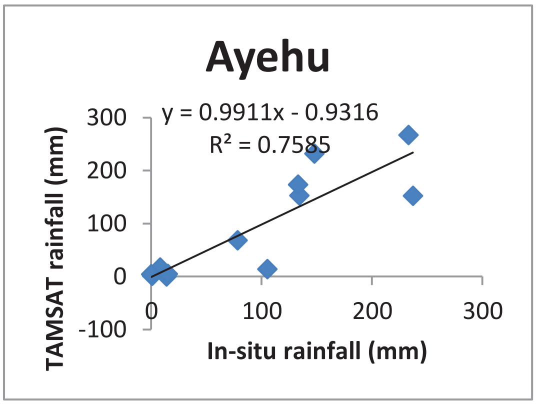


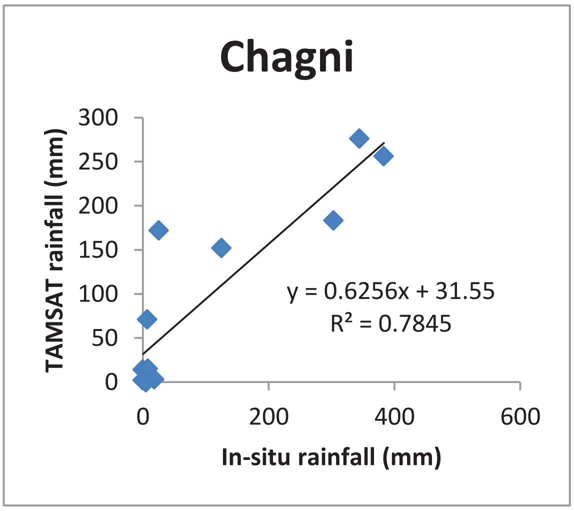


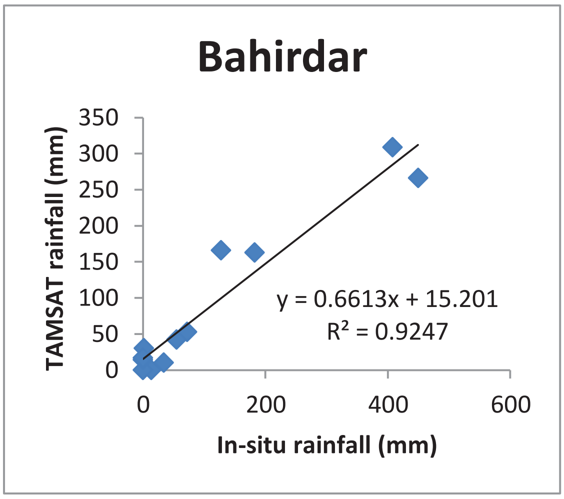

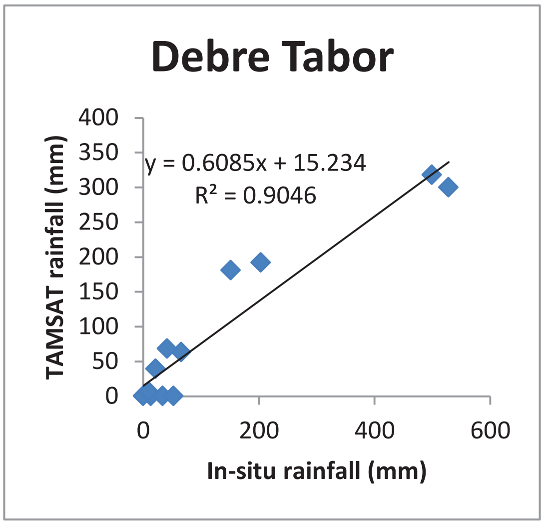
Debre Tabor
y = 0.6085x + 15.234
R² = 0.9046
TAMSAT rainfall (mm)
In-situ rainfall (mm)
0
50
100
150
200
250
300
350
400
0
200
400
600

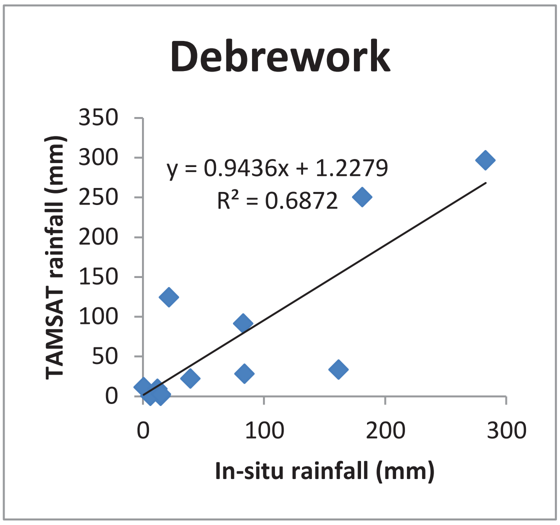
Debrework
y = 0.9436x + 1.2279
R² = 0.6872
TAMSAT rainfall (mm)
In-situ rainfall (mm)
0
50
100
150
200
250
300
350
0
100
200
300

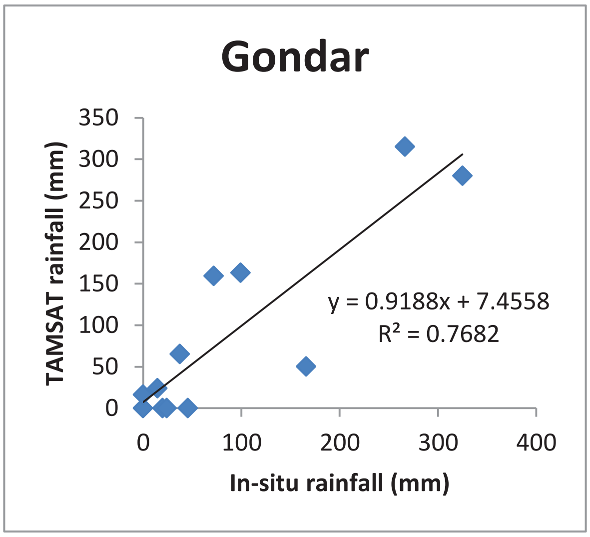
Gondar
y = 0.9188x + 7.4558
R² = 0.7682
TAMSAT rainfall (mm)
In-situ rainfall (mm)
0
50
100
150
200
250
300
350
0
100
200
300
400

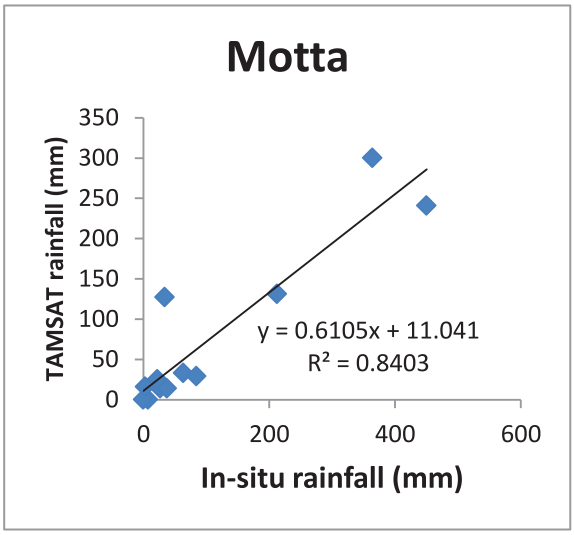
Motta
y = 0.6105x + 11.041
R² = 0.8403
TAMSAT rainfall (mm)
In-situ rainfall (mm)
0
50
100
150
200
250
300
350
0
200
400
600

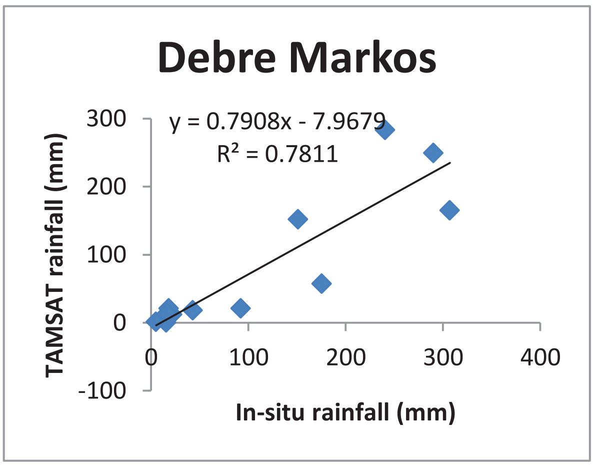
Debre Markos
y = 0.7908x - 7.9679
R² = 0.7811
TAMSAT rainfall (mm)
In-situ rainfall (mm)
-100
0
100
200
300
0
100
200
300
400

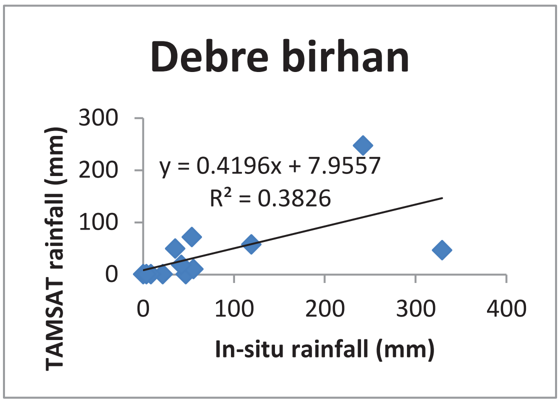
Debre birhan
y = 0.4196x + 7.9557
R² = 0.3826
TAMSAT rainfall (mm)
In-situ rainfall (mm)

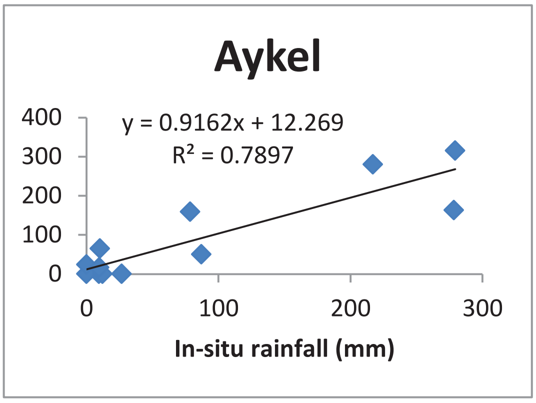
Aykel
y = 0.9162x + 12.269
R² = 0.7897
In-situ rainfall (mm)

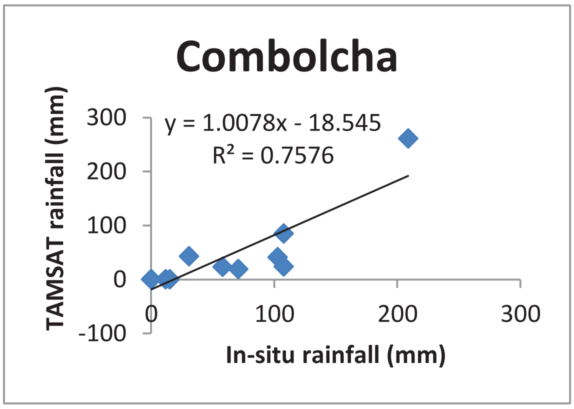
Combolcha
y = 1.0078x - 18.545
R² = 0.7576
TAMSAT rainfall (mm)
In-situ rainfall (mm)

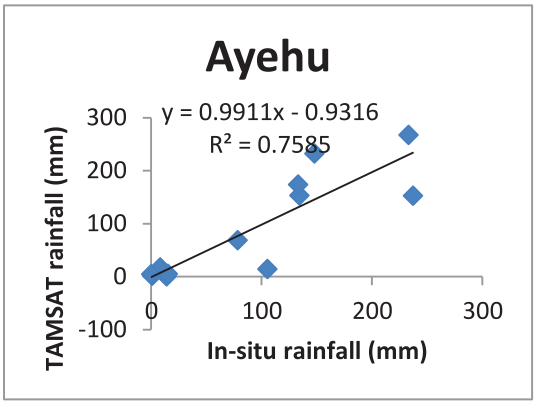
Ayehu
y = 0.9911x - 0.9316
R² = 0.7585
TAMSAT rainfall (mm)
In-situ rainfall (mm)

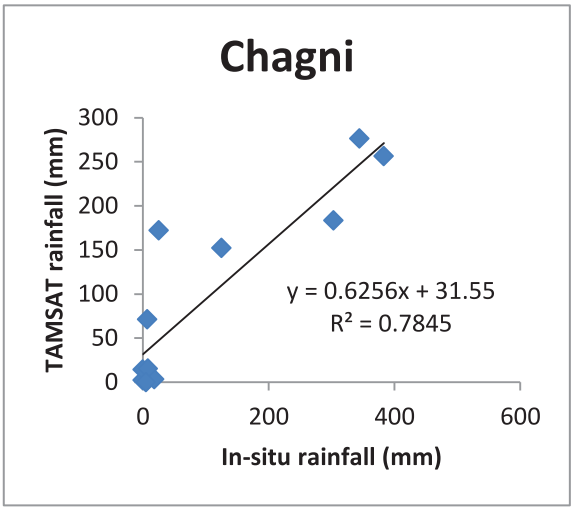
Chagni
y = 0.6256x + 31.55
R² = 0.7845
TAMSAT rainfall (mm)
In-situ rainfall (mm)

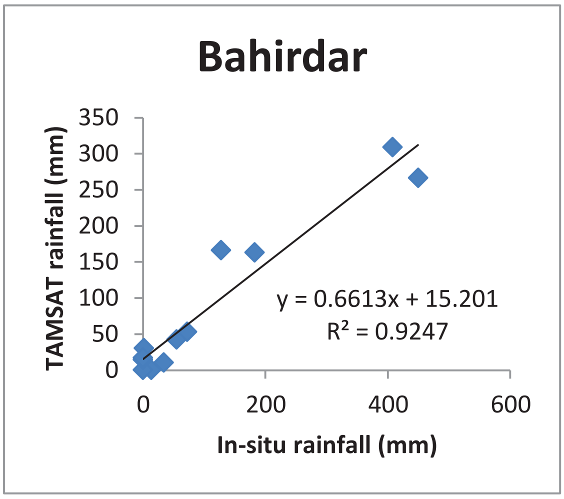
Bahirdar
y = 0.6613x + 15.201
R² = 0.9247
TAMSAT rainfall (mm)
In-situ rainfall (mm)

APPENDEX C: SPIRITS analysis for North Shewa

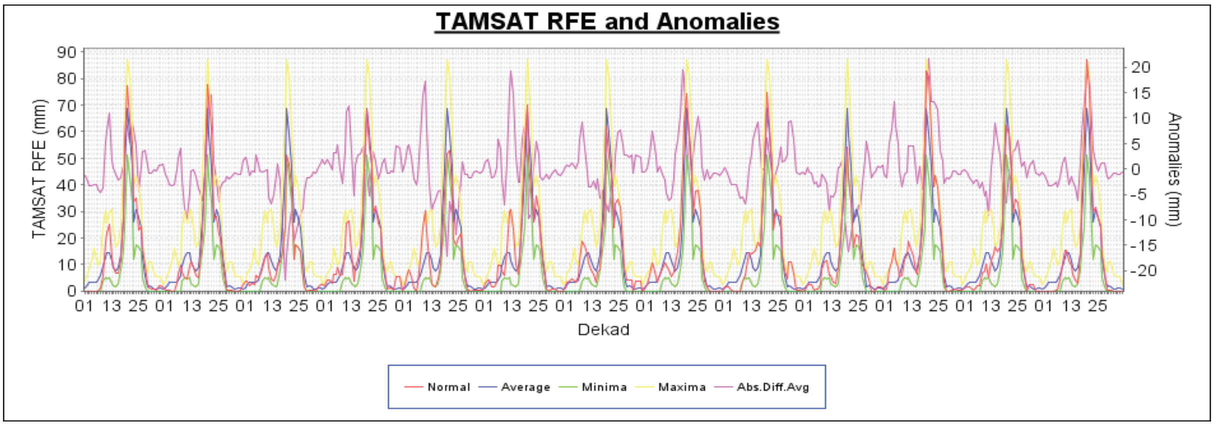


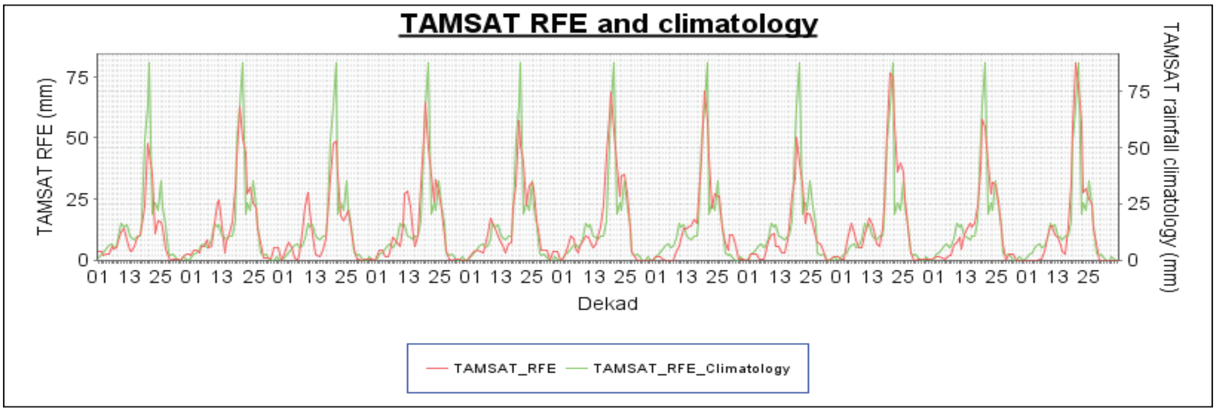


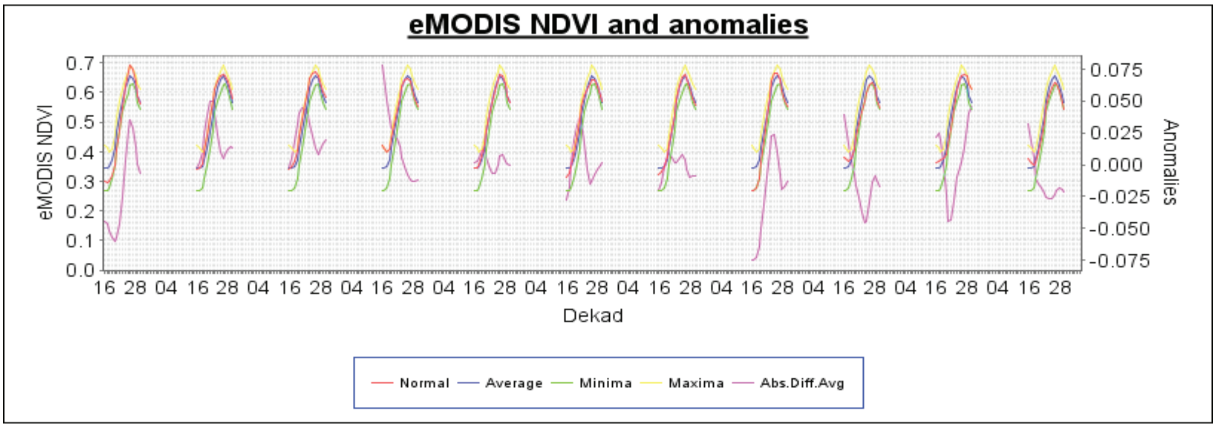


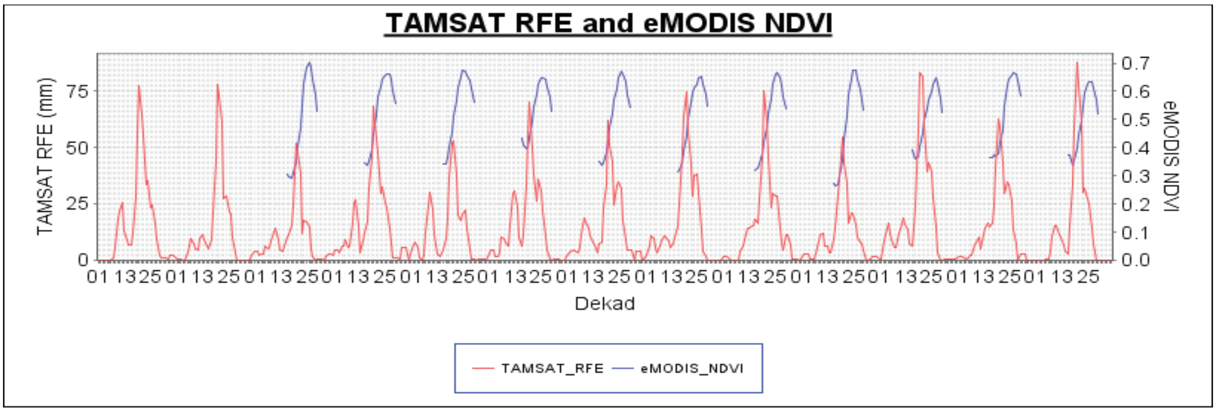

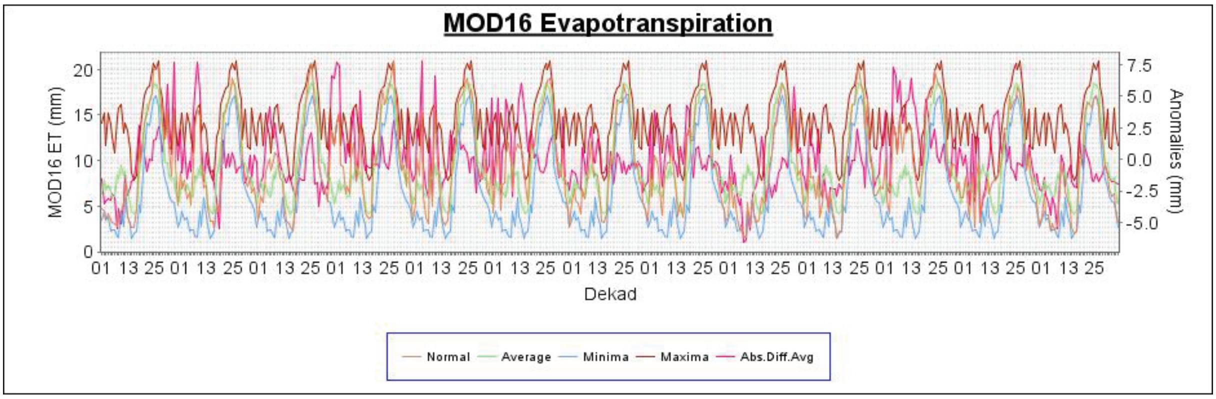
MOD16 Evapotranspiration
MOD16 ET (mm)
Anomalies (mm)
Dekad
Normal
Average
Minima
Maxima
Abs.Diff.Avg

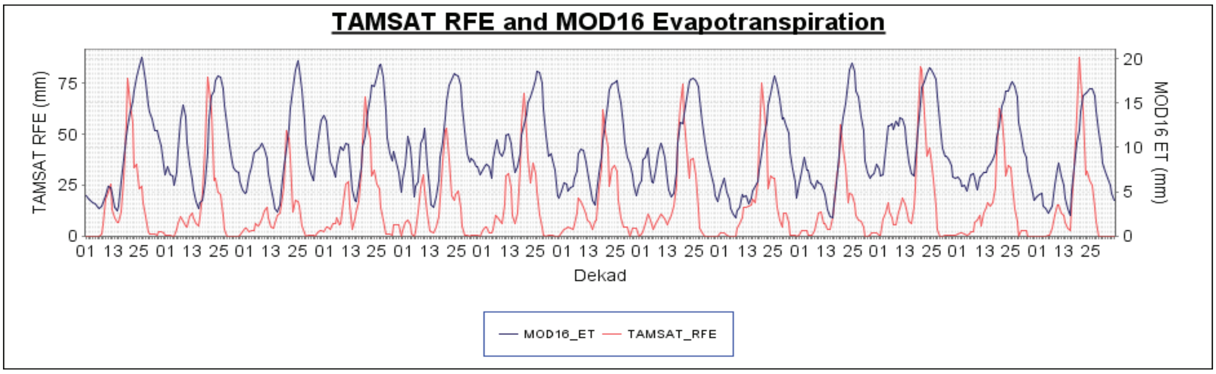
TAMSAT RFE and MOD16 Evapotranspiration
TAMSAT RFE (mm)
MOD16 ET (mm)
Dekad
MOD16_ET
TAMSAT_RFE

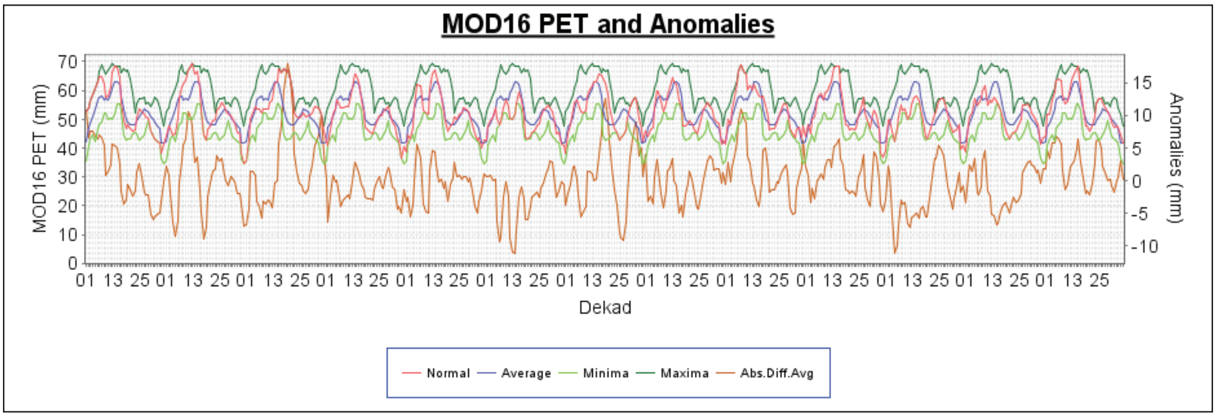
MOD16 PET and Anomalies
MOD16 PET (mm)
Anomalies (mm)
Dekad
Normal
Average
Minima
Maxima
Abs.Diff.Avg

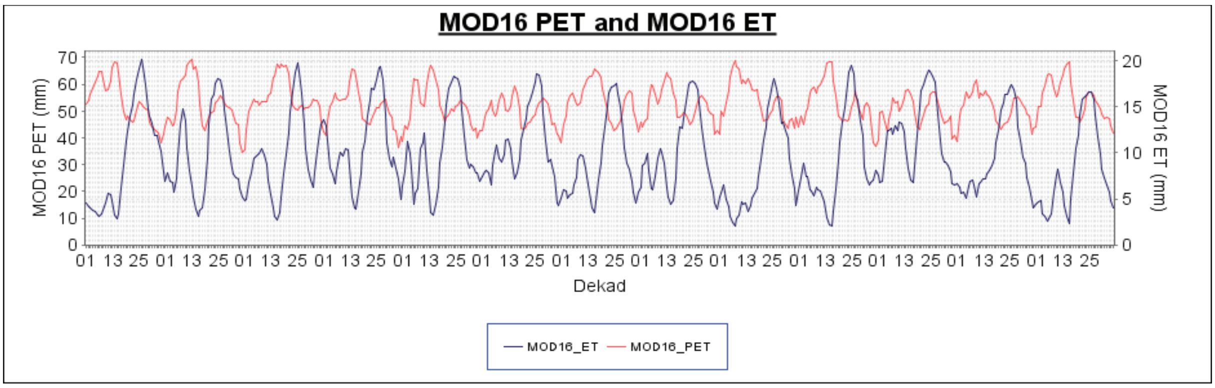
MOD16 PET and MOD16 ET
MOD16 PET (mm)
MOD16 ET (mm)
Dekad
MOD16_ET
MOD16_PET

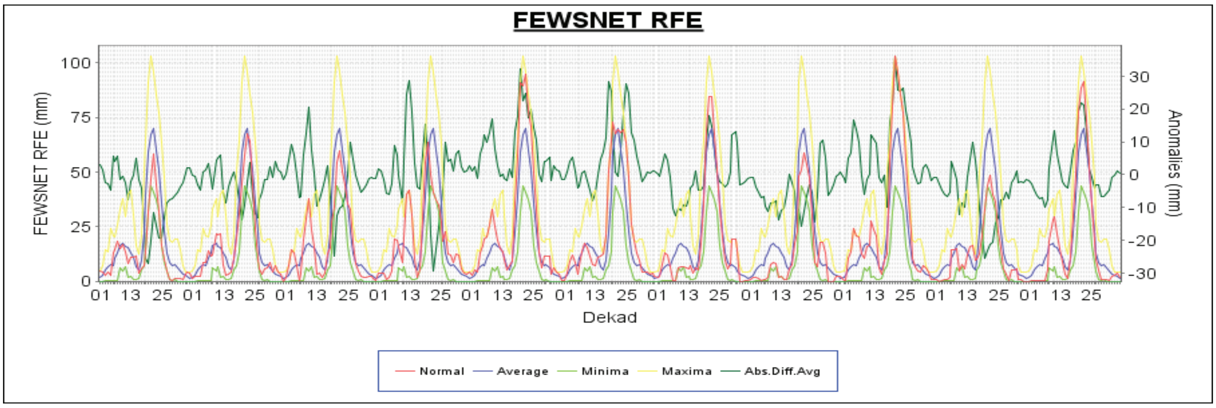
FEWSNET RFE
FEWSNET RFE (mm)
Anomalies (mm)
Dekad
Normal
Average
Minima
Maxima
Abs.Diff.Avg

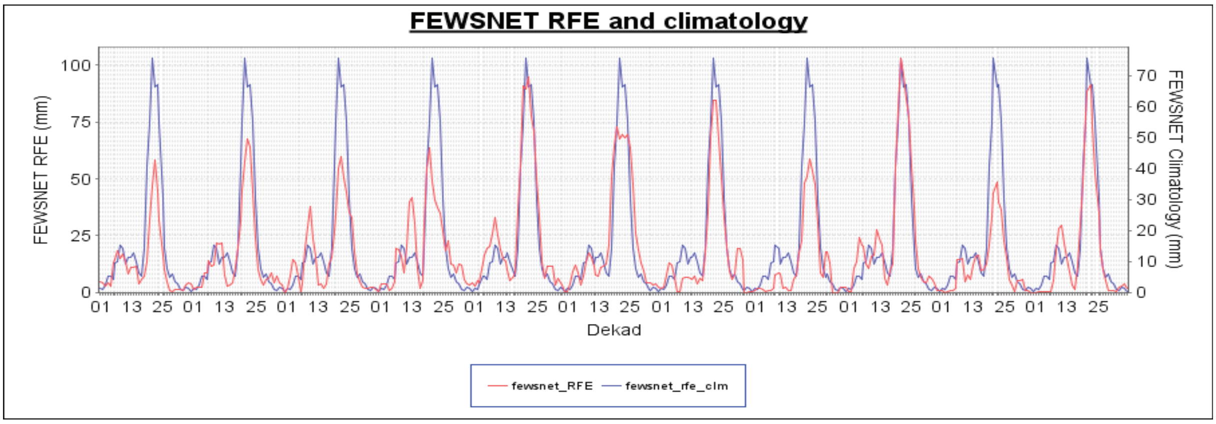
FEWSNET RFE and climatology
FEWSNET RFE (mm)
FEWSNET Climatology (mm)
Dekad
fewsnet_RFE
fewsnet_rfe_clm